

# Revealing Perception and Generation Dynamics in LVLMs: Mitigating Hallucinations via Validated Dominance Correction

Guangtao Lyu<sup>1</sup>, Xinyi Cheng<sup>2</sup>, Chenghao Xu<sup>3</sup>, Qi Liu<sup>1</sup>, Muli Yang<sup>4</sup>, Fen Fang<sup>4</sup>,  
Huilin Chen<sup>5</sup>, Jiexi Yan<sup>2</sup>, Xu Yang<sup>1</sup>, Cheng Deng<sup>1\*</sup>

<sup>1</sup> School of Electronic Engineering, Xidian University, China, <sup>2</sup> School of Computer Science and Technology, Xidian University, China, <sup>3</sup> Hohai university, China, <sup>4</sup> Institute for Infocomm Research (I<sup>2</sup>R), A\*STAR, Singapore, <sup>5</sup>School of Foreign Languages, Xidian University, China,

{guangtaolyu, qiliu, xinyicheng}@stu.xidian.edu.cn, fang.fen@a-star.edu.sg, {jxyan1995, muliyang.xd, xuyang.xd, chdeng.xd}@gmail.com, hlchen@xidian.edu.cn

## Abstract

*Large Vision-Language Models (LVLMs) have shown remarkable capabilities, yet hallucinations remain a persistent challenge. This work presents a systematic analysis of the internal evolution of visual perception and token generation in LVLMs, revealing two key patterns. First, perception follows a three-stage GATE process: early layers perform a Global scan, intermediate layers Approach and Tighten on core content, and later layers Explore supplementary regions. Second, generation exhibits an SAD (Subdominant Accumulation to Dominant) pattern, where hallucinated tokens arise from the repeated accumulation of subdominant tokens lacking support from attention (visual perception) or feed-forward network (internal knowledge). Guided by these findings, we devise the VDC (Validated Dominance Correction) strategy, which detects unsupported tokens and replaces them with validated dominant ones to improve output reliability. Extensive experiments across multiple models and benchmarks confirm that VDC substantially mitigates hallucinations.*

## 1. Introduction

LVLMs have achieved remarkable progress in multimodal reasoning and can handle diverse tasks [1, 5, 47]. However, they often hallucinate, generating content inconsistent with visual inputs or user instructions, which undermines their reliability in safety-critical domains such as medical analysis [10, 27, 65] and autonomous driving [31, 62, 64].

The causes of hallucinations in LVLMs are complex and often attributed to multiple factors [6, 30, 43, 50]. Two aspects have received particular attention. First, models tend

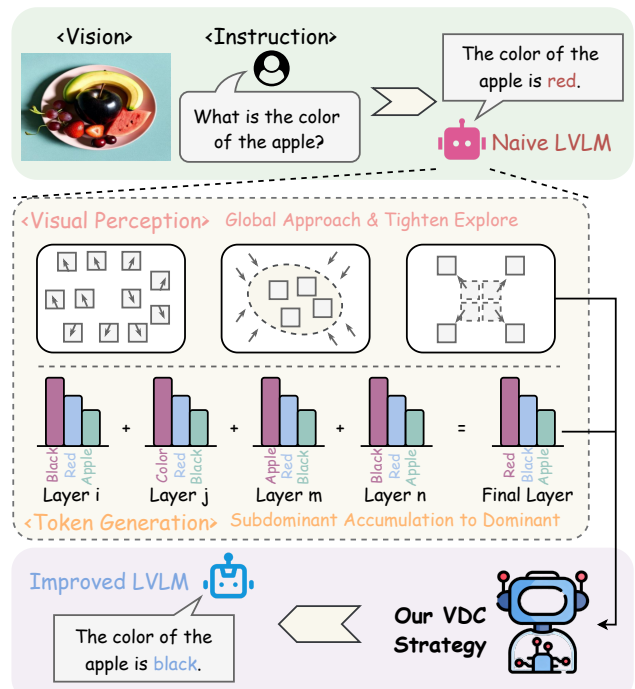


Figure 1. Overview of our framework. We analyze hallucinations via internal perception and generation dynamics, revealing the **GATE (Global, Approach & Tighten, Explore)** pattern in visual perception, the **SAD (Subdominant Accumulation to Dominant)** pattern in token generation, and devise **VDC (Validated Dominance Correction)** strategy to mitigate hallucinations.

to overly rely on textual information, reflected in consistently lower attention to visual tokens compared to text tokens [12, 19, 25, 51, 84]. This observation has motivated methods aimed at increasing visual attention weights [2, 51] or, conversely, reducing them as negative examples to induce hallucinations and contrast against the original input [28, 42, 58]. Second, a perception-generation mis-

\*Corresponding author

match has been observed: even when the model correctly perceives relevant visual content, later outputs can abruptly change, resulting in incorrect tokens [14, 63, 72]. These findings suggest that intermediate layers may provide more reliable signals than the final layers [44, 63], and some works have proposed leveraging intermediate representations to correct corresponding signals in later layers to improve reliability [14, 71, 90].

Although many methods have been proposed to mitigate hallucinations, the underlying mechanisms behind these phenomena remain poorly understood. Why can a model, despite exhibiting relatively low visual attention ratio in the middle layers, still focus accurately on task-relevant regions? And why do errors sometimes emerge in the final layers, even after earlier layers have correctly attended to key visual cues [35, 52, 53, 67, 72]? These questions suggest that static observations of attention ratios or layer-wise outputs are insufficient to explain the model’s behavior. Motivated by this, we take a dynamic and evolutionary perspective, systematically examining how visual perception and token generation evolve across layers to uncover the internal processes underlying hallucination formation.

To investigate how LVLMs perceive multimodal inputs, we analyze the evolution of visual attention across layers using complementary tools. We introduce two analytical perspectives, stage-to-global and inter-stage attention difference maps, to reveal the internal attention dynamics. Our analysis uncovers a structured three-stage process, termed **GATE (Global, Approach and Tighten, Explore)**. In the *Global* stage, attention is broadly distributed across the image for holistic exploration. During the *Approach and Tighten* stages, it progressively focuses on task-relevant regions and suppresses peripheral cues, often reducing overall attention ratios despite improved grounding. In the final *Explore* stage, attention redistributes toward complementary regions for validation and refinement before generation. The GATE pattern explains why intermediate layers may show lower visual attention ratios while still achieving accurate grounding, as the model tightens its focus after understanding the instruction.

We further investigate the internal evolution of token generation by adopting the logit lens [57] to project hidden states onto the vocabulary space. Beyond the whole-layer view, we analyze submodules, including the attention and feed-forward network (FFN), where the attention reflects *visual perception* [42, 51] and the FFN encodes *internal parametric knowledge* [15, 22, 34, 80]. This intra-layer analysis reveals how perception and knowledge jointly shape token distributions. We find that early layers exhibit token fluctuations, while middle layers gradually stabilize semantically coherent candidates, consistent with the GATE perception pattern. We further identify the **SAD (Subdominant Accumulation to Dominant)** pattern, in which hal-

lucinated tokens never appear as dominant (rank-1) candidates in either the attention or FFN outputs. Instead, they persist as subdominant candidates across multiple layers and progressively accumulate through cross-layer aggregation, eventually overtaking the originally correct tokens. This provides a mechanistic explanation for why LVLMs may “see correctly but speak wrongly” [35, 52] and suggests a practical diagnostic cue: tokens that never dominate attention or FFN outputs are likely unreliable and can be replaced by previously validated dominant tokens.

Motivated by the GATE and SAD patterns, we introduce **Validated Dominance Correction (VDC)**, a training-free, plug-and-play strategy for detecting and mitigating hallucinations. VDC validates each generated token by checking whether it is dominant in either the attention output (visual perception) or the FFN output (internal knowledge) at any layer. Tokens that fail this validation are replaced with the most frequently dominant token across layers, ensuring that each output is supported by at least visual perception or internal knowledge. VDC effectively suppresses unreliable tokens and enhances output reliability. Extensive experiments confirm its effectiveness in reducing hallucinations and validating our internal dynamic analysis.

In summary, this work makes three key contributions:

- We perform a multi-perspective analysis within each internal LVLM layer, jointly examining attention and FFN outputs to understand how perception and generation dynamically evolve and how hallucinations arise.
- We discover two patterns, GATE for perception and SAD for generation, which elucidate the evolution of visual perception and token generation, offering mechanistic insights into hallucination formation.
- We propose VDC, a training-free, plug-and-play method that uses validated dominant token to correct invalidated one, mitigating hallucinations across benchmarks.

## 2. Related Work

**LVLMs.** The success of LLMs [4, 13, 17, 54, 59, 68] has enabled LVLMs [1, 3, 5, 16, 26, 47, 49, 81, 89], which integrate visual and textual information for multimodal understanding and reasoning. Typical LVLMs use a pre-trained visual encoder to extract image features, projected into the LLM embedding space via linear layers or Q-Former modules [11, 48, 79], and then combined with textual inputs. LVLMs achieve strong performance in various tasks [27, 31, 45, 56, 78, 81, 89]. Despite these advances, hallucination remains a major challenge [23, 41, 50, 75].

**Hallucinations in LVLMs.** Hallucinations refer to content that is irrelevant, factually incorrect, or inconsistent with visual inputs [33, 50, 84]. Their emergence in LVLMs is complex, influenced by multiple factors [6, 50]. A common issue is over reliance on textual information [20, 51], often reflected in lower attention to visual tokens; prior

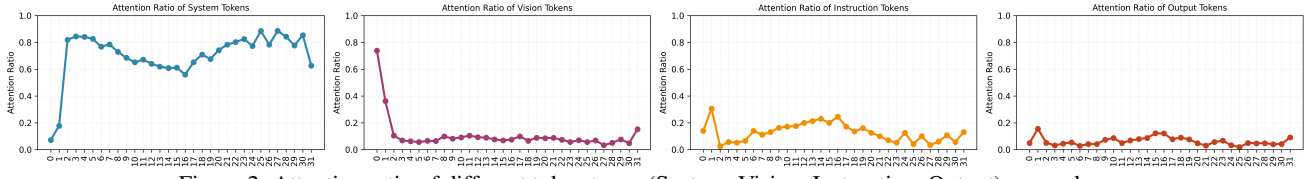


Figure 2. Attention ratio of different token types (System, Vision, Instruction, Output) across layers.

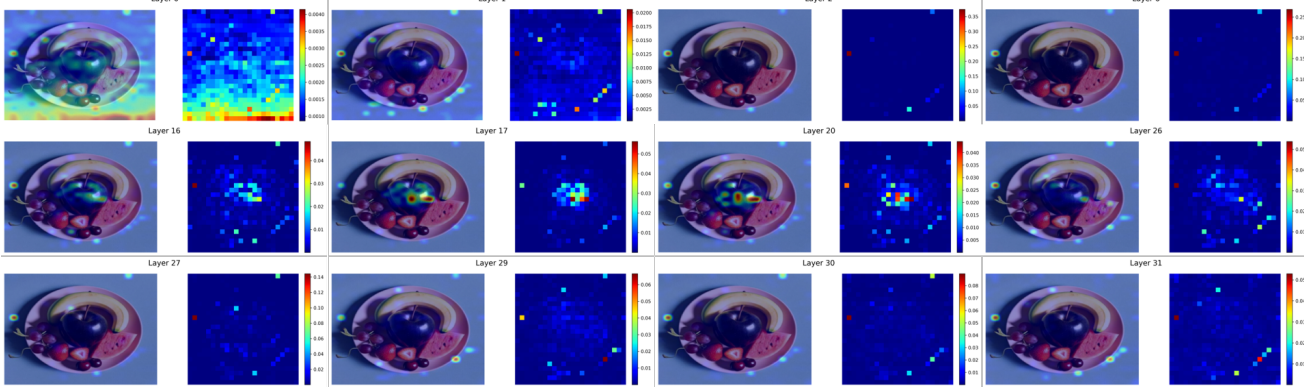


Figure 3. Visual attention heatmaps across layers.

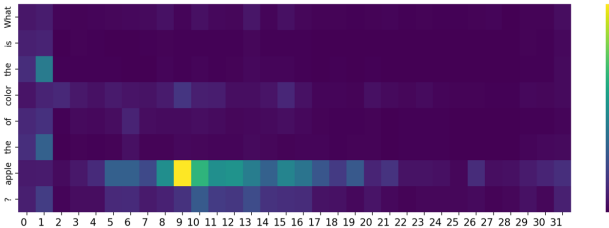


Figure 4. Instruction attention heatmaps across layers.

works address this by increasing visual attention [28, 29, 51, 58, 77] or using reduced visual attention as negative examples [2, 20, 32, 42]. Another key observation is the perception-generation mismatch: even when visual content is correctly perceived, outputs may produce incorrect tokens [35, 63, 67, 72]. Some studies leverage middle layers to improve final predictions [14, 44, 71] or selectively skip late layers [18, 86, 90]. Despite these efforts, understanding remains limited. We study hallucinations through internal perception and generation dynamics, identifying the GATE pattern in visual perception, the SAD pattern in token generation, and proposing VDC to mitigate hallucinations.

### 3. Analysis of LVLM Internal Dynamics

**Preliminaries.** We denote the system message tokens, visual tokens, instruction tokens, and output tokens as  $\mathbf{X}_s$ ,  $\mathbf{X}_v$ ,  $\mathbf{X}_i$ , and  $\mathbf{X}_o$ , respectively [47]. Each LVLM layer [69] consists of an attention module, an FFN, and normalization modules. We denote the hidden states of the attention mod-

ule, FFN, and the layer as  $h^{\text{attn}}$ ,  $h^{\text{ffn}}$ , and  $h$ :

$$h^{\text{attn}} = \text{Attention}(\text{Norm}(h)), \quad (1)$$

$$h = h + h^{\text{attn}}, \quad (2)$$

$$h^{\text{ffn}} = \text{FFN}(\text{Norm}(h)), \quad (3)$$

$$h = h + h^{\text{ffn}}. \quad (4)$$

We apply *logits lens* [57] to project them into the language space for an internal examination of token generation.

### 3.1. Perception: The GATE Pattern

**Layer-Wise Attention Dynamics.** To understand how LVLMs perceive and integrate multimodal information, we analyze the evolution of visual and textual attention across layers using both qualitative and quantitative approaches. Specifically, we visualize the layer-wise attention ratio across four token groups: system, vision, instruction, and output (Fig. 2), as well as the attention from generation tokens to visual and instruction tokens (Figs. 3, 4).

From Figs. 2, 3, 4, we observe changes in both attention spatial focus and allocation across layers. In the first two layers, attention over visual tokens is widespread, covering nearly the entire image, indicating a global scanning process. At layer 3, attention to system tokens increases sharply while attention to other token types decreases. Between layers 3 and 16, both visual and instruction attentions increase steadily, as the model understands key instruction cues and focuses on the corresponding visual regions. Attention to the instruction peaks around layer 16, while at layer 17 visual attention concentrates on the main object region. From layers 17 to 26, attention tightens on key object regions while peripheral regions receive less focus, slightly lowering overall visual and instruction ratios. At layer 27,

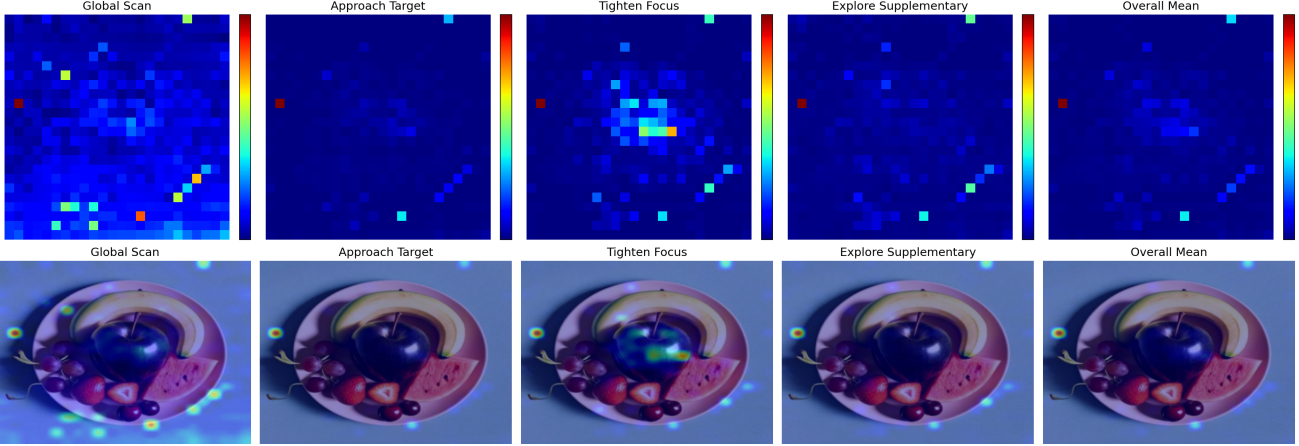


Figure 5. Heatmaps of visual attention across different stages, illustrating the GATE pattern (Global–Approach&Tighten–Explore). In the Global stage, the model attends broadly to the entire image; in the Approach phase, attention gradually shifts toward the apple region; during the Tighten phase, focus converges tightly on the apple; and in the final Explore stage, attention expands again to nearby areas.

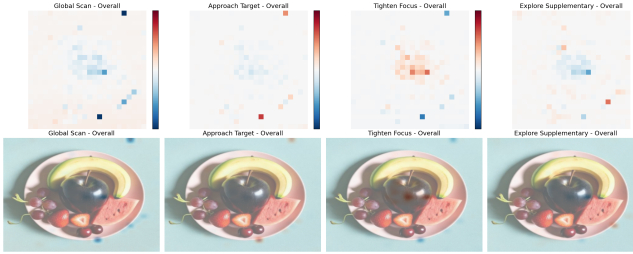


Figure 6. Stage-to-global attention difference maps, showing how each stage’s attention deviates from the overall average, highlighting stage-specific focus or deficiencies.

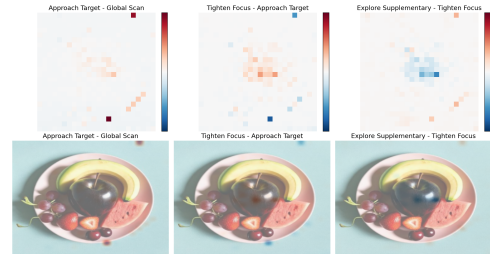


Figure 7. Inter-stage attention difference maps, showing how attention shifts across consecutive stages, revealing the model’s dynamic focus evolution and the sequence of information integration.

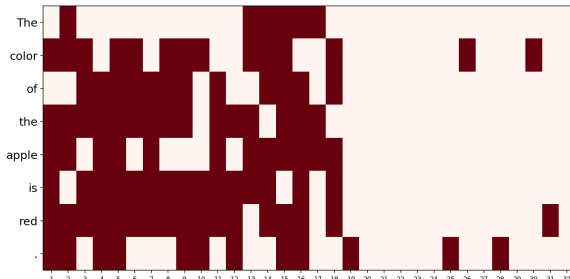


Figure 8. Dominant (Top-1) token changes across layers. Red means changes from the previous layer, white means no change.

attention in the key region begins to disperse, shifting toward complementary regions. In the final layer, visual and instruction attentions show a rebound.

**Stage-Level Interpretation and Visualization.** Building on the layer-wise attention dynamics, we summarize the evolving perception process into three stages, forming the GATE pattern (Global, Approach & Tighten, Explore), which reflects systematic shifts in spatial focus and task-relevant allocation across layers. To illustrate these stages, we visualize representative stage-specific attention maps (Fig. 5), compute stage-to-global differences to highlight emphasized or suppressed regions (Fig. 6), and analyze

inter-stage differences to capture the transitions between consecutive stages (Fig. 7). Such differential visualizations also help mitigate the effect of attention sinks [36, 61, 66, 76], providing a clearer and more interpretable depiction of stage-wise evolution. Additional examples are provided in Appendix Figs. 13, 14, 15, 16, 17, 18, 19, and 20.

In the *Global Scanning* stage, attention is broadly distributed across the image, characterized by high visual ratios. Stage-to-global difference maps highlight stronger attention in surrounding regions (red) and weaker attention at the center (blue), reflecting a holistic scanning process. In the *Approach & Tighten* stage, the model begins integrating textual guidance and gradually approaches task-relevant regions, directing increased attention to key objects, such as the apple, as shown by the difference maps (red). It then tightens its focus on the most informative object and instruction tokens, while suppressing peripheral areas (center red, surroundings blue), demonstrating refined attention to critical cues. In the *Explore Supplementary* stage, attention expands to peripheral or complementary regions. Difference maps reveal reduced focus on previously attended key regions (blue) alongside increased attention to secondary areas (red), reflecting a rechecking process that reassesses surrounding regions while retaining critical information.

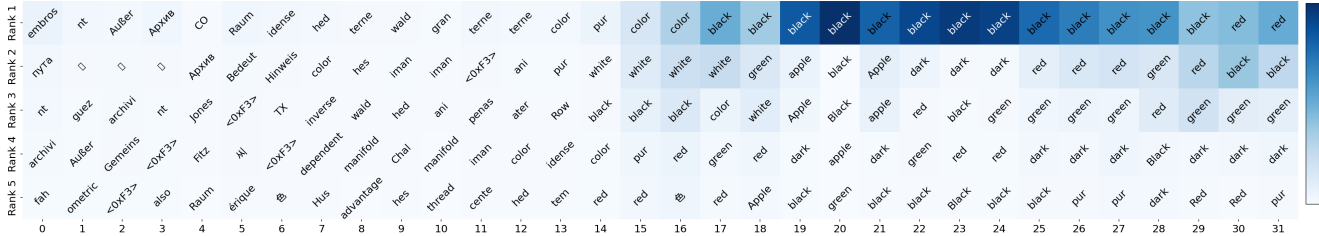


Figure 9. Top-5 tokens from layer outputs. Early layers exhibit rapid token fluctuations, followed by a stable phase producing the correct token “black”. The last two layers show a sudden shift to the incorrect token “red”.

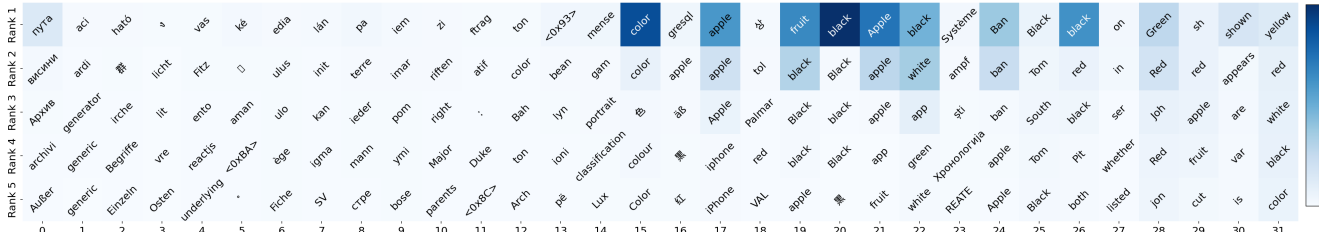


Figure 10. Top-5 tokens from attention outputs. The token “red” does not appear as the dominant (rank-1) token in any layer, indicating that it fails to receive support or validation from visual perception.

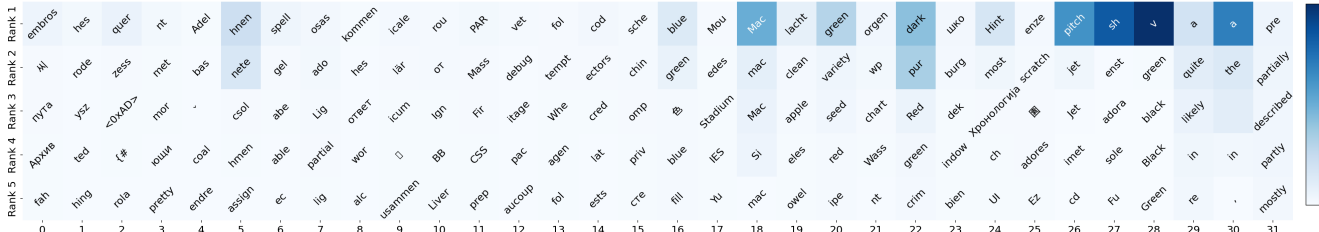


Figure 11. Top-5 tokens from FFN outputs. The token “red” also does not appear as the dominant (rank-1) token in any layer, indicating that it also fails to receive support or validation from the model’s internal parametric knowledge.

**The GATE Pattern.** The GATE characterizes how attention is dynamically allocated and reallocated across layers in LVLMs. However, even when the model correctly attends to core visual regions, it can still generate incorrect outputs, revealing a perception–generation mismatch [35, 52]. To uncover the source of this discrepancy, we next analyze the token generation process in detail.

### 3.2. Generation: The SAD Pattern

**Layer-Wise Generation Analysis.** As shown by the GATE analysis, even when LVLMs achieve correct visual grounding, they can still produce hallucinated outputs. To investigate this perception–generation mismatch, we perform a layer-wise analysis of token predictions using the *logit-lens* [57], projecting hidden states into the vocabulary space (Fig 9). We also track whether the rank-1 (dominant) token changes across layers (Figs 8), standardizing all tokens to lowercase to ignore superficial syntactic differences and focus on semantic changes (see Appendix Figs. 13, 14, 15, 16, 17, 18, 19, and 20 for more examples).

In Fig. 9, during the early layers, corresponding to the Global and Approach stages of the GATE, predicted tokens are largely unrelated to the target, gradually transitioning

from random content words to task-relevant terms, such as color attributes. Around layer 17, the model begins to predict the correct token “black,” coinciding with the peak instruction attention (Fig. 2) and the visual focus on the “black apple” region (Fig. 3). The token “black” remains dominant throughout the middle layers, covering the entire Tighten stage, until the final two layers, where it abruptly shifts to the incorrect token “red”.

In Fig. 8, early layers exhibit frequent token fluctuations, corresponding roughly to the Global Scanning and early Approach phases, during which the model broadly explores the image and interprets the user instruction. By the middle layers, simple structural tokens such as “of”, “apple”, “object”, and “image” begin to stabilize, indicating that basic and simple words are resolved relatively early. In contrast, content-rich tokens such as “red”, “brick”, “side”, and “walk” continue to fluctuate, reflecting higher uncertainty and a greater need for semantic reasoning.

These observations indicate that intermediate layers already stabilize low-level or simple tokens. Tokens that consistently appear as the dominant prediction across multiple layers can be considered resolved, suggesting potential computational efficiency gains by skipping these tokens in

subsequent processing [18, 37, 55, 61]. In contrast, tokens that continue to fluctuate across layers likely reflect higher uncertainty and a greater need for semantic reasoning. This variability provides an informative signal for identifying challenging samples and can guide dataset curation or selection, focusing training or evaluation on instances where persistent token changes occur [7, 9, 73].

In the final two layers, token predictions often change. For example, a token like “black” replaced with “red”, or “side” become “brick”. These late-stage shifts occur in both correct and hallucinated outputs, indicating that such sudden changes are an inherent property of LVLMs.

**Disentangling Intra-Layer Generation Dynamics.** To understand why these abrupt changes occur, we further disentangle the contributions of attention and FFN within each layer. By examining the projected outputs  $\mathbf{X}_o^{\text{attn}}$  and  $\mathbf{X}_o^{\text{ffn}}$  separately, we can trace how visually grounded perception and internal knowledge independently influence token generation, and how their interactions lead to sudden token shifts in the final output.

Figs. 10, 11, and 9 show that  $\mathbf{X}_o^{\text{attn}}$  and  $\mathbf{X}_o^{\text{ffn}}$  changes rapidly across layers, while the whole layer output  $\mathbf{X}_o$  remains comparatively stable. The final hallucinated token “red” never appears as dominant in either branch, instead remaining subdominant tokens that gradually overtakes the correct token in  $\mathbf{X}_o$  via multi-layer accumulation.

Across many examples (Figs. 13, 14, 15, 16, 17, 18, 19, and 20 in Appendix), we observe that late-stage token shifts are common. Correct tokens that have previously appeared as dominant in attention or FFN outputs, such as “brick”, typically remain grounded, while hallucinated tokens that never dominate can gradually accumulate across layers and replace correct tokens in the final output.

**The SAD Pattern.** We term this the **SAD** (*Subdominant Accumulation to Dominant*). It describes how hallucinated tokens, which never become the dominant token in either the attention or FFN outputs, remain consistently subdominant across layers yet gradually accumulate, eventually overtaking the correct token in the final output. This provides a mechanistic explanation for why LVLMs may “see correctly but speak wrongly” and suggests a practical diagnostic cue: tokens that never dominate in either the attention output (visual perception) or the FFN output (internal knowledge) are likely unreliable and can be replaced by previously validated dominant tokens.

## 4. Validated Dominance Correction

Motivated by the SAD and GATE patterns, we propose **Validated Dominance Correction (VDC)**, a training-free plug-and-play strategy to detecting and mitigate hallucination. In essence, if a generated token never appears as the dominant token in either the attention (visual perception) or FFN (internal knowledge) outputs, it is considered unreliable and treated as a hallucination. Such tokens are immediately replaced with a validated token that has been dominant in at least one output within the current generation step, ensuring that every token in the output is grounded in either visual perception or knowledge-based reasoning.

---

### Algorithm 1 Validated Dominance Correction (VDC)

---

**Require:** Dominant tokens  $d_t^{\text{attn},\ell}, d_t^{\text{ffn},\ell}$ ; output  $\mathbf{X}_o$

**Ensure:** Corrected output  $\hat{\mathbf{X}}_o$

```

1: Initialize  $\hat{\mathbf{X}}_o \leftarrow \{\}$ 
2: for  $t = 1$  to  $T$  do
3:   Generate token  $\mathbf{x}_t$ 
4:   Collect dominant tokens  $\{d_t^{\text{attn},\ell}, d_t^{\text{ffn},\ell}\}_{\ell=1}^L$ 
5:   if  $\mathbf{x}_t \notin \{d_t^{\text{attn},\ell}, d_t^{\text{ffn},\ell} \forall \ell\}$  then
6:     Mark  $\mathbf{x}_t$  as hallucinated
7:     Replace  $\mathbf{x}_t \leftarrow \mathbf{x}_t^*$ , the most frequent dominant token across layers
8:   end if
9:   Append  $\mathbf{x}_t$  to  $\hat{\mathbf{X}}_o$ 
10: end for
11: return  $\hat{\mathbf{X}}_o$ 

```

---

able and treated as a hallucination. Such tokens are immediately replaced with a validated token that has been dominant in at least one output within the current generation step, ensuring that every token in the output is grounded in either visual perception or knowledge-based reasoning.

Let  $\mathbf{X}_o = \{\mathbf{x}_1, \dots, \mathbf{x}_T\}$  denote the sequence of generated tokens. At each generation step  $t$ , we obtain layer-wise dominant tokens from attention and FFN modules, denoted by  $d_t^{\text{attn},\ell}$  and  $d_t^{\text{ffn},\ell}$  for  $\ell = 1, \dots, L$ . A generated token  $\mathbf{x}_t$  is considered *validated* if it appears as the dominant token in either output at any layer:

$$\text{validated}(\mathbf{x}_t) = \begin{cases} 1, & \exists \ell \text{ s.t. } \mathbf{x}_t = d_t^{\text{attn},\ell} \text{ or } \mathbf{x}_t = d_t^{\text{ffn},\ell} \\ 0, & \text{otherwise.} \end{cases} \quad (5)$$

If  $\text{validated}(\mathbf{x}_t) = 0$ , the token is treated as a hallucination and replaced by the most frequent dominant token  $\mathbf{x}_t^*$  across layers:

$$\mathbf{x}_t^* = \arg \max_{\mathbf{x} \in \{d_t^{\text{attn},\ell}, d_t^{\text{ffn},\ell}\}} \sum_{\ell=1}^L \mathbb{I}[\mathbf{x} = d_t^{\text{attn},\ell} \text{ or } \mathbf{x} = d_t^{\text{ffn},\ell}]. \quad (6)$$

The corrected output is updated online as:

$$\hat{\mathbf{x}}_t = \begin{cases} \mathbf{x}_t, & \text{if } \text{validated}(\mathbf{x}_t) = 1 \\ \mathbf{x}_t^*, & \text{if } \text{validated}(\mathbf{x}_t) = 0 \end{cases}, \quad t = 1, \dots, T. \quad (7)$$

## 5. Experiments

**Benchmarks.** We evaluate on three standard hallucination benchmarks: (1) **POPE** [43], which measures object-level hallucinations through binary yes/no questions about object existence. (2) **CHAIR** [60], which assesses hallucinations in open-ended image captioning on 500 randomly selected images from the MSCOCO [46] validation set. The metric is mainly reported at both instance-level (CHAIR<sub>I</sub>) and sentence-level

Table 1. Results on the POPE.  $\uparrow$  indicates higher is better. The best and second results are **bolded** and underlined.

Setup	Method	LLaVA-1.5				InstructBLIP				Qwen-VL			
		Acc. $\uparrow$	Prec. $\uparrow$	Rec. $\uparrow$	F1 $\uparrow$	Acc. $\uparrow$	Prec. $\uparrow$	Rec. $\uparrow$	F1 $\uparrow$	Acc. $\uparrow$	Prec. $\uparrow$	Rec. $\uparrow$	F1 $\uparrow$
Random	Vanilla	84.63	83.07	87.00	84.99	83.33	82.38	84.80	83.57	85.17	97.22	72.40	83.00
	Vanilla + VDC	<u>84.90</u>	83.24	87.40	<u>85.27</u>	83.70	82.68	<u>85.27</u>	83.95	85.73	97.35	73.47	83.74
	VCD	84.57	82.59	87.60	85.02	84.60	85.12	83.87	84.49	87.37	97.14	77.00	85.91
	VCD + VDC	<u>84.93</u>	83.00	87.87	85.36	85.23	85.78	84.47	85.12	88.00	97.34	78.13	86.69
	M3ID	86.33	85.30	87.80	86.53	85.00	84.72	85.40	85.06	86.03	<u>97.87</u>	73.67	84.06
	M3ID + VDC	<u>86.73</u>	85.83	88.00	86.90	85.53	85.34	85.80	85.57	86.50	<b>97.90</b>	74.60	84.68
	ONLY	<u>89.57</u>	90.68	88.20	89.42	86.13	86.04	86.27	86.15	<u>89.63</u>	95.70	<u>83.00</u>	88.90
	ONLY + VDC	<b>89.83</b>	<b>90.73</b>	<b>88.73</b>	<b>89.72</b>	<b>86.50</b>	<b>86.14</b>	<b>87.00</b>	<b>86.57</b>	<b>90.07</b>	95.74	<b>83.87</b>	<b>89.41</b>
Popular	Vanilla	81.33	78.14	87.00	82.33	76.00	72.11	84.80	77.94	84.50	94.73	73.07	82.50
	Vanilla + VDC	<u>81.80</u>	78.77	87.07	82.71	76.47	72.56	85.13	78.34	84.67	94.91	73.27	82.69
	VCD	80.80	77.11	87.60	82.02	77.20	74.00	83.87	78.62	85.83	94.02	76.53	84.38
	VCD + VDC	<u>81.20</u>	77.56	87.80	82.36	77.23	<u>74.04</u>	83.87	78.65	85.90	94.18	76.53	84.44
	M3ID	82.30	79.10	87.80	83.22	77.23	73.41	85.40	78.95	85.43	<u>95.94</u>	74.00	83.55
	M3ID + VDC	<u>82.97</u>	79.77	<u>88.33</u>	83.83	<u>77.67</u>	73.80	<u>85.80</u>	<u>79.35</u>	85.67	<b>96.12</b>	74.33	83.83
	ONLY	<u>86.10</u>	<u>84.64</u>	88.20	<u>86.39</u>	77.50	73.40	<b>86.27</b>	79.31	87.70	91.92	<u>82.67</u>	<u>87.05</u>
	ONLY + VDC	<b>86.83</b>	<b>85.39</b>	<b>88.87</b>	<b>87.10</b>	<b>78.40</b>	<b>74.54</b>	<b>86.27</b>	<b>79.98</b>	<b>88.03</b>	92.29	<b>83.00</b>	<b>87.40</b>
Adversarial	Vanilla	75.87	71.18	86.93	78.27	74.17	70.04	84.47	76.58	82.53	90.80	72.40	80.56
	Vanilla + VDC	<u>76.63</u>	72.01	87.13	<u>78.85</u>	74.97	70.96	84.53	77.15	83.20	91.09	73.60	81.42
	VCD	75.23	70.23	87.60	77.96	75.80	<u>72.29</u>	83.67	77.56	83.10	88.46	76.13	81.83
	VCD + VDC	<u>75.67</u>	70.52	<u>88.20</u>	78.38	<u>76.30</u>	<b>72.82</b>	83.93	77.98	83.73	88.98	77.00	82.56
	M3ID	76.63	71.79	87.73	78.97	75.40	71.26	85.13	77.58	83.03	<u>91.12</u>	73.20	81.18
	M3ID + VDC	<u>76.87</u>	72.05	87.80	79.15	<u>76.30</u>	72.20	85.53	<u>78.30</u>	83.40	<b>91.34</b>	73.80	81.64
	ONLY	<u>79.43</u>	<u>75.07</u>	88.13	<u>81.08</u>	75.63	71.28	<u>85.87</u>	77.90	<u>83.77</u>	85.10	<u>81.87</u>	<u>83.45</u>
	ONLY + VDC	<b>79.67</b>	<b>75.23</b>	<b>88.47</b>	<b>81.31</b>	<b>76.40</b>	72.02	<b>86.33</b>	<b>78.53</b>	<b>84.40</b>	85.78	<b>82.47</b>	<b>84.09</b>

Table 2. Results on CHAIR.  $\downarrow$  denotes lower is better. \* denotes results reported in prior works [28, 70, 71]. – denotes unavailable results.

Method	LLaVA-1.5				InstructBLIP				Qwen-VL			
	Max Token 64		Max Token 128		Max Token 64		Max Token 128		Max Token 64		Max Token 128	
	CHAIR <sub>S</sub> $\downarrow$	CHAIR <sub>I</sub> $\downarrow$										
Vanilla	26.5	9.4	55.1	16.4	31.5	11.4	57.4	17.6	33.8	12.9	52.1	16.7
Vanilla + VDC	<u>15.6</u>	<u>6.2</u>	33.6	9.8	<u>21.4</u>	<u>8.1</u>	38.2	9.1	19.4	8.4	<u>34.2</u>	<u>9.1</u>
VCD	24.8	8.0	54.4	16.6	30.0	10.1	60.7	18.0	33.3	13.1	50.4	17.2
VCD + VDC	<u>19.3</u>	7.1	32.9	<u>9.2</u>	24.2	8.6	38.6	9.7	<u>19.1</u>	8.8	34.6	9.6
M3ID	21.4	6.4	56.6	15.8	31.1	10.5	62.3	18.2	32.3	11.9	49.8	17.4
M3ID + VDC	<u>15.3</u>	<u>6.1</u>	<u>33.8</u>	9.6	<u>21.6</u>	9.2	<u>33.9</u>	<u>8.9</u>	19.2	<u>8.1</u>	34.2	9.7
ONLY	20.1	6.3	51.2	14.9	23.9	8.3	52.5	15.7	27.7	8.6	48.1	14.4
ONLY + VDC	<b>13.6</b>	<b>5.6</b>	<b>31.4</b>	<b>8.9</b>	<b>17.8</b>	<b>6.6</b>	<b>31.6</b>	<b>7.3</b>	<b>17.8</b>	<b>7.4</b>	<b>32.6</b>	<b>8.7</b>
DOLA*	–	–	47.8	13.8	–	–	48.4	15.9	–	–	46.8	12.9
DeCo*	–	–	37.8	11.1	–	–	41.2	12.4	–	–	42.2	10.4
OPERA*	–	–	44.6	12.8	–	–	46.4	14.2	–	–	–	–
Woodpecker*	24.9	7.5	57.6	16.7	31.2	10.8	60.8	17.6	31.1	12.3	51.8	16.3
HALC*	21.7	7.1	51.0	14.8	24.5	8.0	53.8	15.7	28.2	9.1	49.6	15.4

(CHAIR<sub>S</sub>): CHAIR<sub>I</sub> =  $\frac{|\{\text{hallucinated objects}\}|}{|\{\text{all objects}\}|}$ , CHAIR<sub>S</sub> =  $\frac{|\{\text{captions containing hallucinations}\}|}{|\{\text{captions}\}|}$ . (3) **MME** [21], which provides a comprehensive evaluation across four subsets—*existence*, *count*, *position*, and *color*—covering both object-level and attribute-level hallucinations.

**Evaluated LVLMs.** Following prior works [42, 70], we evaluate VDC on three open-source LVLMs: **LLaVA-1.5** [47], **InstructBLIP** [16], and **Qwen-VL** [5]. Unless specified, we use **LLaVA-1.5** as the default model.

**Baselines.** We compare VDC with the following approaches: Vanilla, VCD [42], M3ID [20], and ONLY [70]. Vanilla denotes the standard LVLML decoding strategy,

where the next token is directly sampled from the post-softmax probability distribution following prior works [42, 70]. VCD contrasts the logits between the original and noisy images. M3ID contrasts the logits from inputs with and without visual information. ONLY leverages the text-to-vision entropy ratio of each word to selectively amplify visually grounded textual cues. **More LVLMs and Baselines are shown in Appendix. B**

**Implementation Details.** Our VDC is a *plug-and-play* strategy that integrates seamlessly into existing LVLMs and mitigation strategies, requiring only validation and correction of final tokens. Unlike contrastive decoding methods

Table 3. Results on MME.  $\uparrow$  indicates higher is better.

Method	Object-level		Attribute-level		MME Score $\uparrow$
	Existence $\uparrow$	Count $\uparrow$	Position $\uparrow$	Color $\uparrow$	
Vanilla	185.00	126.67	128.33	148.33	588.33
Vanilla + VDC	187.00	128.67	130.33	150.67	596.67
VCD	185.00	136.67	128.33	158.33	608.33
VCD + VDC	186.00	138.33	131.67	159.67	615.67
M3ID	190.00	136.67	128.33	158.33	613.33
M3ID + VDC	<b>191.00</b>	138.33	130.67	<b>160.33</b>	<u>620.33</u>
ONLY	190.00	143.33	133.33	148.33	614.99
ONLY + VDC	<b>191.00</b>	<u>144.67</u>	<u>134.67</u>	150.33	<b>620.67</b>

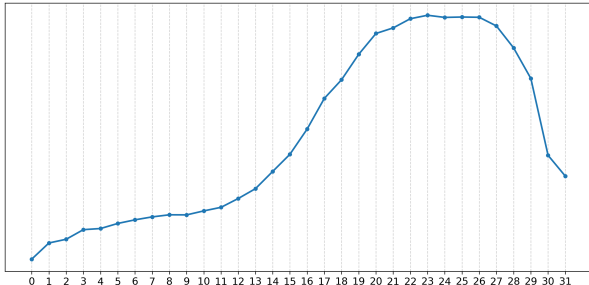


Figure 12. Frequency distribution of layers where the validated correction tokens appear during VDC on CHAIR Benchmark.

needing multiple forward passes, VDC collects multi-layer logits in a single pass and performs VDC through efficient tensor operations. It thus achieves near inference speed to vanilla decoding with consistently improved reliability. All experiments are conducted on a single NVIDIA RTX A6000 GPU (48GB).

## 5.1. Main Experimental Results

**Results on POPE.** As shown in Tab. 1, integrating our VDC into different baselines consistently improves performance across various LVLM backbones and evaluation settings, demonstrating its robustness and general applicability.

**Results on MME.** As shown in Tab. 3, incorporating VDC into existing baselines consistently improves both object-level metrics (Existence, Count) and attribute-level metrics (Position, Color), indicating that VDC enhances the model’s overall multimodal understanding.

**Results on CHAIR.** On the open-ended CHAIR benchmark (Tab. 2), integrating VDC into different models significantly reduces hallucination rates across all settings. The improvement is particularly pronounced for longer generation sequences (128 tokens), where hallucinations tend to accumulate. This demonstrates that identifying unsupported tokens and replacing them with validated ones yields more faithful and visually grounded outputs. Fig. 12 shows the layer-wise frequency of tokens used for correction. While some correction tokens appear across multiple layers, their occurrences are notably concentrated after layer 17, corresponding to the *Tighten* phase identified by the GATE analysis. These results further validate our analysis of the internal perception and generation dynamics of LVLM.

Table 4. Ablation results on validation sources.

Validation Sources	$\text{CHAIR}_S \downarrow$	$\text{CHAIR}_I \downarrow$	Recall $\uparrow$
Baseline	55.1	16.4	<b>70.6</b>
Layer-only	47.1	11.3	64.2
Attn+FFN	<b>33.6</b>	<b>9.8</b>	<u>69.9</u>
Attn+FFN+Layer	44.2	<u>10.6</u>	68.4

Table 5. Ablation results on correction sources.

Correction Sources	$\text{CHAIR}_S \downarrow$	$\text{CHAIR}_I \downarrow$	Recall $\uparrow$
Baseline	55.1	16.4	<b>70.6</b>
Layer-only	46.3	11.6	64.2
Attn+FFN	<b>26.2</b>	<b>8.6</b>	44.6
Attn+FFN+Layer	<u>33.6</u>	<u>9.8</u>	<u>69.9</u>

## 5.2. Ablation Studies

**Validation Sources.** We evaluate the impact of different validation sources by using dominant tokens from Layer-only, Attn+FFN, and Attn+FFN+Layer. As shown in Tab. 4, Attn+FFN consistently achieves the lowest hallucination rates, whereas including layer outputs (Attn+FFN+Layer) increases the hallucination rate. This increase can be attributed to the *SAD pattern*, where subdominant incorrect tokens gradually accumulate to dominate, causing some hallucinated tokens to be mistakenly considered validated and thereby amplifying hallucinations. In contrast, using Attn+FFN means a token needs to appear in either visual perception or internal knowledge to be considered validated, providing a more precise criterion for reliability.

**Correction Sources.** We evaluate the impact of different sources on VDC performance by testing corrections using dominant tokens from Layer-only, Attn+FFN, and Attn+FFN+Layer. As shown in Tab. 5, using Attn+FFN for replacement achieves the lowest hallucination rates, indicating that cross-stream attention and FFN signals provide the most precise corrections. Including the whole layer output (Attn+FFN+Layer) increases recall but slightly raises hallucination rates, suggesting that layer outputs help coverage at the expense of precision. To balance correction accuracy and coverage, we adopt Attn+FFN+Layer as the default source for VDC.

**Skipping Early Layers.** We evaluate whether early layers contribute meaningfully to VDC. To this end, we skip the first 2, 10, and 16 layers in both validation and correction sources. As shown in Tab. 6, skipping these layers has negligible impact on hallucination rates. Analysis of perception and generation dynamics reveals that early layers mainly produce unstable or semantically uninformative tokens, consistent with the *Global* and *Approach* phases in the GATE pattern, during which the model is still interpreting the instruction and gradually attending to relevant regions. These findings suggest that the first ten layers can be safely excluded, improving efficiency while confirming that the GATE pattern effectively guides VDC optimization.

Table 6. Ablation on skipping early layers in VDC.

Skipped Early Layers	$\text{CHAIR}_S \downarrow$	$\text{CHAIR}_I \downarrow$	Recall $\uparrow$
None (Full)	33.6	9.8	69.9
2 layers	33.6	9.8	69.9
10 layers	33.6	9.8	69.9
16 layers	33.4	10.1	69.6

## 6. Conclusion

In this work, we systematically analyze the perception-generation dynamics of LVLMs. We uncover the **GATE** (Global, Approach & Tighten, Explore) pattern in visual perception and the **SAD** (Subdominant Accumulation to Dominant) pattern in token generation, revealing how hallucinations emerge from subdominant token accumulation. Based on these insights, we propose **VDC** (Validated Dominance Correction), a lightweight strategy to reliably detect and mitigate hallucinations.

## References

[1] Josh Achiam, Steven Adler, Sandhini Agarwal, Lama Ahmad, Ilge Akkaya, Florencia Leoni Aleman, Diogo Almeida, Janko Altenschmidt, Sam Altman, Shyamal Anadkat, et al. Gpt-4 technical report. *arXiv:2303.08774*, 2023. 1, 2

[2] Wenbin An, Feng Tian, Sicong Leng, Jiahao Nie, Haonan Lin, QianYing Wang, Ping Chen, Xiaoqin Zhang, and Shijian Lu. Mitigating object hallucinations in large vision-language models with assembly of global and local attention. In *CVPR*, 2025. 1, 3

[3] Anthropic. Introducing Claude 3.5 Sonnet. 2024. Announcement of Claude 3.5 Sonnet model release, featuring improved intelligence, vision capabilities, and new Artifacts feature. 2

[4] Jinze Bai, Shuai Bai, Yunfei Chu, Zeyu Cui, Kai Dang, Xiaodong Deng, Yang Fan, Wenbin Ge, Yu Han, Fei Huang, et al. Qwen technical report. *arXiv:2309.16609*, 2023. 2

[5] Jinze Bai, Shuai Bai, Shusheng Yang, Shijie Wang, Sinan Tan, Peng Wang, Junyang Lin, Chang Zhou, and Jingren Zhou. Qwen-vl: A frontier large vision-language model with versatile abilities. *arXiv:2308.12966*, 2023. 1, 2, 7

[6] Zechen Bai, Pichao Wang, Tianjun Xiao, Tong He, Zongbo Han, Zheng Zhang, and Mike Zheng Shou. Hallucination of multimodal large language models: A survey. *arXiv:2404.18930*, 2024. 1, 2

[7] Hritik Bansal, Devandra Singh Sachan, Kai-Wei Chang, Aditya Grover, Gargi Ghosh, Wen-tau Yih, and Ramakanth Pasunuru. Honeybee: Data recipes for vision-language reasoners. *arXiv:2510.12225*, 2025. 6, 1

[8] Freya Behrens, Luca Biggio, and Lenka Zdeborová. Understanding counting in small transformers: The interplay between attention and feed-forward layers. In *ICML*, 2024. 1

[9] Ellis Brown, Jihan Yang, Shusheng Yang, Rob Fergus, and Saining Xie. Benchmark designers should “train on the test set” to expose exploitable non-visual shortcuts. *arXiv:2511.04655*, 2025. 6, 1

[10] Junying Chen, Chi Gui, Ruyi Ouyang, Anningzhe Gao, Shunian Chen, Guiming Hardy Chen, Xidong Wang, Zhenyang Cai, Ke Ji, Xiang Wan, et al. Towards injecting medical visual knowledge into multimodal llms at scale. In *NeurIPS*, 2024. 1

[11] Zhe Chen, Jiannan Wu, Wenhui Wang, Weijie Su, Guo Chen, Sen Xing, Muyan Zhong, Qinglong Zhang, Xizhou Zhu, Lewei Lu, et al. Internvl: Scaling up vision foundation models and aligning for generic visual-linguistic tasks. In *CVPR*, 2024. 2

[12] Zhaorun Chen, Zhuokai Zhao, Hongyin Luo, Huaxiu Yao, Bo Li, and Jiawei Zhou. Halc: Object hallucination reduction via adaptive focal-contrast decoding. *arXiv:2403.00425*, 2024. 1

[13] Wei-Lin Chiang, Zhuohan Li, Zi Lin, Ying Sheng, Zhang-hao Wu, Hao Zhang, Lianmin Zheng, Siyuan Zhuang, Yong-hao Zhuang, Joseph E. Gonzalez, Ion Stoica, and Eric P. Xing. Vicuna: An open-source chatbot impressing gpt-4 with 90%\* chatgpt quality, 2023. 2

[14] Yung-Sung Chuang, Yujia Xie, Hongyin Luo, Yoon Kim, James Glass, and Pengcheng He. Dola: Decoding by contrasting layers improves factuality in large language models. In *ICLR*, 2023. 2, 3, 1

[15] Damai Dai, Li Dong, Yaru Hao, Zhifang Sui, Baobao Chang, and Furu Wei. Knowledge neurons in pretrained transformers. In *ACL*, 2022. 2

[16] Wenliang Dai, Junnan Li, Dongxu Li, Anthony Tiong, Junqi Zhao, Weisheng Wang, Boyang Li, Pascale N Fung, and Steven Hoi. Instructclip: Towards general-purpose vision-language models with instruction tuning. *NeurIPS*, 2023. 2, 7

[17] DeepSeek-AI, Daya Guo, Dejian Yang, Haowei Zhang, Junxiao Song, et al. Deepseek-r1: Incentivizing reasoning capability in llms via reinforcement learning, 2025. 2

[18] Maha Elbayad, Jiatao Gu, Edouard Grave, and Michael Auli. Depth-adaptive transformer. *arXiv:1910.10073*, 2019. 3, 6, 1

[19] Alessandro Favero, Luca Zancato, Matthew Trager, Siddharth Choudhary, Pramuditha Perera, Alessandro Achille, Ashwin Swaminathan, and Stefano Soatto. Multi-modal hallucination control by visual information grounding. In *CVPR*, 2024. 1

[20] Alessandro Favero, Luca Zancato, Matthew Trager, Siddharth Choudhary, Pramuditha Perera, Alessandro Achille, Ashwin Swaminathan, and Stefano Soatto. Multi-modal hallucination control by visual information grounding. In *CVPR*, 2024. 2, 3, 7

[21] Chaoyou Fu, Peixian Chen, Yunhang Shen, Yulei Qin, Mengdan Zhang, Xu Lin, Zhenyu Qiu, Wei Lin, Jinrui Yang, Xiawu Zheng, et al. Mme: A comprehensive evaluation benchmark for multimodal large language models. *arXiv:2306.13394*, 2023. 7

[22] Mor Geva, Roei Schuster, Jonathan Berant, and Omer Levy. Transformer feed-forward layers are key-value memories. In *EMNLP*, 2021. 2

[23] Anisha Gunjal, Jihan Yin, and Erhan Bas. Detecting and preventing hallucinations in large vision language models. In *AAAI*, 2024. 2

[24] Jinghan He, Kuan Zhu, Haiyun Guo, Junfeng Fang, Zhenglin Hua, Yuheng Jia, Ming Tang, Tat-Seng Chua, and Jinqiao Wang. Cracking the code of hallucination in l1lms with vision-aware head divergence. In *ACL*, 2025. 1

[25] Nanxing Hu, Xiaoyue Duan, Jinchao Zhang, and Guoliang Kang. Enhancing visual reliance in text generation: A bayesian perspective on mitigating hallucination in large vision-language models. In *ACMMM*, 2025. 1

[26] Shengding Hu, Yuge Tu, Xu Han, Chaoqun He, Ganqu Cui, Xiang Long, Zhi Zheng, Yewei Fang, Yuxiang Huang, Weilin Zhao, et al. Minicpm: Unveiling the potential of small language models with scalable training strategies. *arXiv:2404.06395*, 2024. 2

[27] Yutao Hu, Tianbin Li, Quanfeng Lu, Wenqi Shao, Junjun He, Yu Qiao, and Ping Luo. Omnimedvqa: A new large-scale comprehensive evaluation benchmark for medical l1lm. In *CVPR*, 2024. 1, 2

[28] Qidong Huang, Xiaoyi Dong, Pan Zhang, Bin Wang, Conghui He, Jiaqi Wang, Dahua Lin, Weiming Zhang, and

Nenghai Yu. Opera: Alleviating hallucination in multi-modal large language models via over-trust penalty and retrospection-allocation. *arXiv:2311.17911*, 2023. 1, 3, 7

[29] Fushuo Huo, Wenchao Xu, Zhong Zhang, Haozhao Wang, Zhicheng Chen, and Peilin Zhao. Self-introspective decoding: Alleviating hallucinations for large vision-language models. *arXiv:2408.02032*, 2024. 3

[30] Ziwei Ji, Nayeon Lee, Rita Frieske, Tiezheng Yu, Dan Su, Yan Xu, Etsuko Ishii, Ye Jin Bang, Andrea Madotto, and Pascale Fung. Survey of hallucination in natural language generation. *ACM Computing Surveys*, 2023. 1

[31] Bo Jiang, Shaoyu Chen, Bencheng Liao, Xingyu Zhang, Wei Yin, Qian Zhang, Chang Huang, Wenyu Liu, and Xinggang Wang. Senna: Bridging large vision-language models and end-to-end autonomous driving. *arXiv:2410.22313*, 2024. 1, 2

[32] Nicholas Jiang, Anish Kachinthaya, Suzanne Petryk, and Yossi Gandelsman. Interpreting and editing vision-language representations to mitigate hallucinations. In *ICLR*. 3

[33] Zhangqi Jiang, Junkai Chen, Beier Zhu, Tingjin Luo, Yankun Shen, and Xu Yang. Devils in middle layers of large vision-language models: Interpreting, detecting and mitigating object hallucinations via attention lens. In *CVPR*, 2025. 2

[34] Shibo Jie, Yehui Tang, Ning Ding, Zhi-Hong Deng, Kai Han, and Yunhe Wang. Memory-space visual prompting for efficient vision-language fine-tuning. *arXiv:2405.05615*, 2024. 2

[35] Ryo Kamoi, Yusen Zhang, Sarkar Sniidha Sarathi Das, Ranran Haoran Zhang, and Rui Zhang. Visonlyqa: Large vision language models still struggle with visual perception of geometric information. *arXiv:2412.00947*, 2024. 2, 3, 5

[36] Seil Kang, Jinyeong Kim, Junhyeok Kim, and Seong Jae Hwang. See what you are told: Visual attention sink in large multimodal models. *arXiv:2503.03321*, 2025. 4

[37] Wei-Tsung Kao, Tsung-Han Wu, Po-Han Chi, Chun-Cheng Hsieh, and Hung-Yi Lee. Bert’s output layer recognizes all hidden layers? some intriguing phenomena and a simple way to boost bert. *arXiv:2001.09309*, 2020. 6, 1

[38] Junho Kim, Hyunjung Kim, Kim Yeonju, and Yong Man Ro. Code: Contrasting self-generated description to combat hallucination in large multi-modal models. *NeurIPS*, 2024. 1

[39] Goro Kobayashi, Tatsuki Kurabayashi, Sho Yokoi, and Kentaro Inui. Incorporating residual and normalization layers into analysis of masked language models. *arXiv:2109.07152*, 2021. 1

[40] Goro Kobayashi, Tatsuki Kurabayashi, Sho Yokoi, and Kentaro Inui. Analyzing feed-forward blocks in transformers through the lens of attention maps. In *ICLR*, 2025. 1

[41] Katherine Lee, Orhan Firat, Ashish Agarwal, Clara Fanjiang, and David Sussillo. Hallucinations in neural machine translation. 2018. 2

[42] Sicong Leng, Hang Zhang, Guanzheng Chen, Xin Li, Shijian Lu, Chunyan Miao, and Lidong Bing. Mitigating object hallucinations in large vision-language models through visual contrastive decoding. In *CVPR*, 2024. 1, 2, 3, 7

[43] Yifan Li, Yifan Du, Kun Zhou, Jinpeng Wang, Wayne Xin Zhao, and Ji-Rong Wen. Evaluating object hallucination in large vision-language models. *arXiv:2305.10355*, 2023. 1, 6

[44] Zhuowei Li, Haizhou Shi, Yunhe Gao, Di Liu, Zhenting Wang, Yuxiao Chen, Ting Liu, Long Zhao, Hao Wang, and Dimitris N Metaxas. The hidden life of tokens: Reducing hallucination of large vision-language models via visual information steering. In *ICML*, 2025. 2, 3

[45] Bin Lin, Yang Ye, Bin Zhu, Jiaxi Cui, Munan Ning, Peng Jin, and Li Yuan. Video-llava: Learning united visual representation by alignment before projection. In *EMNLP*, 2024. 2

[46] Tsung-Yi Lin, Michael Maire, Serge Belongie, James Hays, Pietro Perona, Deva Ramanan, Piotr Dollár, and C Lawrence Zitnick. Microsoft coco: Common objects in context. In *ECCV*, 2014. 6

[47] Haotian Liu, Chunyuan Li, Qingyang Wu, and Yong Jae Lee. Visual instruction tuning. In *NeurIPS*, 2023. 1, 2, 3, 7

[48] Haotian Liu, Chunyuan Li, Yuheng Li, and Yong Jae Lee. Improved baselines with visual instruction tuning. In *CVPR*, 2024. 2

[49] Haotian Liu, Chunyuan Li, Yuheng Li, Bo Li, Yuanhan Zhang, Sheng Shen, and Yong Jae Lee. Llavanext: Improved reasoning, ocr, and world knowledge, 2024. 2, 1

[50] Hanchao Liu, Wenyuan Xue, Yifei Chen, Dapeng Chen, Xiutian Zhao, Ke Wang, Liping Hou, Rongjun Li, and Wei Peng. A survey on hallucination in large vision-language models. *arXiv:2402.00253*, 2024. 1, 2

[51] Shi Liu, Kecheng Zheng, and Wei Chen. Paying more attention to image: A training-free method for alleviating hallucination in llms. *arXiv:2407.21771*, 2024. 1, 2, 3

[52] Yexin Liu, Zhengyang Liang, Yueze Wang, Xianfeng Wu, Feilong Tang, Muyang He, Jian Li, Zheng Liu, Harry Yang, Sernam Lim, et al. Unveiling the ignorance of mllms: Seeing clearly, answering incorrectly. In *CVPR*, 2025. 2, 5

[53] Zhining Liu, Ziyi Chen, Hui Liu, Chen Luo, Xianfeng Tang, Suhang Wang, Joy Zeng, Zhenwei Dai, Zhan Shi, Tianxin Wei, et al. Seeing but not believing: Probing the disconnect between visual attention and answer correctness in llms. *arXiv:2510.17771*, 2025. 2

[54] Haoyu Lu, Wen Liu, Bo Zhang, Bingxuan Wang, Kai Dong, Bo Liu, Jingxiang Sun, Tongzheng Ren, Zhuoshu Li, Yaofeng Sun, et al. Deepseek-vl: towards real-world vision-language understanding. *arXiv:2403.05525*, 2024. 2

[55] Xuan Luo, Weizhi Wang, and Xifeng Yan. Adaptive layer-skipping in pre-trained llms. *arXiv:2503.23798*, 2025. 6

[56] Guangtao Lyu, Chenghao Xu, Jieyi Yan, Muli Yang, and Cheng Deng. Towards unified human motion-language understanding via sparse interpretable characterization. In *ICLR*, 2025. 2

[57] Nostalgebraist. Interpreting gpt: the logit lens, 2020. 2, 3, 5

[58] Woohyeon Park, Woojin Kim, Jaeik Kim, and Jaeyoung Do. Second: Mitigating perceptual hallucination in vision-language models via selective and contrastive decoding. In *ICML*, 2025. 1, 3

[59] Alec Radford, Karthik Narasimhan, Tim Salimans, Ilya Sutskever, et al. Improving language understanding by generative pre-training. *OpenAI blog*, 2018. 2

[60] Anna Rohrbach, Lisa Anne Hendricks, Kaylee Burns, Trevor Darrell, and Kate Saenko. Object hallucination in image captioning. *arXiv:1809.02156*, 2018. 6

[61] Tal Schuster, Adam Fisch, Jai Gupta, Mostafa Dehghani, Dara Bahri, Vinh Tran, Yi Tay, and Donald Metzler. Confident adaptive language modeling. *NeurIPS*, 2022. 4, 6, 1

[62] Hao Shao, Yuxuan Hu, Letian Wang, Guanglu Song, Steven L Waslander, Yu Liu, and Hongsheng Li. Lmdrive: Closed-loop end-to-end driving with large language models. In *CVPR*, 2024. 1

[63] Oscar Skean, Md Rifat Arefin, Dan Zhao, Niket Nikul Patel, Jalal Naghiyev, Yann LeCun, and Ravid Shwartz-Ziv. Layer by layer: Uncovering hidden representations in language models. In *ICML*, 2025. 2, 3

[64] Fengzhao Sun, Jun Yu, Yunxiang Zhang, Jiaming Hou, Xilong Lu, Heng Song, and Fang Gao. Towards robust autonomous driving: Conditional multimodal large language models for fine-grained perception. In *ICRA*, 2025. 1

[65] Guohao Sun, Can Qin, Huazhu Fu, Linwei Wang, and Zhiqiang Tao. Self-training large language and vision assistant for medical question answering. *NeurIPS*, 2024. 1

[66] Mingjie Sun, Xinlei Chen, J Zico Kolter, and Zhuang Liu. Massive activations in large language models. *arXiv:2402.17762*, 2024. 4

[67] Shengbang Tong, Zhuang Liu, Yuexiang Zhai, Yi Ma, Yann LeCun, and Saining Xie. Eyes wide shut? exploring the visual shortcomings of multimodal llms. In *CVPR*, 2024. 2, 3

[68] Hugo Touvron, Thibaut Lavril, Gautier Izacard, Xavier Martinet, Marie-Anne Lachaux, Timothée Lacroix, Baptiste Rozière, Naman Goyal, Eric Hambro, Faisal Azhar, et al. Llama: Open and efficient foundation language models. *arXiv:2302.13971*, 2023. 2

[69] Ashish Vaswani, Noam Shazeer, Niki Parmar, Jakob Uszkoreit, Llion Jones, Aidan N Gomez, Łukasz Kaiser, and Illia Polosukhin. Attention is all you need. *NeurIPS*, 2017. 3

[70] Zifu Wan, Ce Zhang, Silong Yong, Martin Q Ma, Simon Stepputtis, Louis-Philippe Morency, Deva Ramanan, Katia Sycara, and Yaqi Xie. Only: One-layer intervention sufficiently mitigates hallucinations in large vision-language models. *arXiv:2507.00898*, 2025. 7

[71] Chenxi Wang, Xiang Chen, Ningyu Zhang, Bozhong Tian, Haoming Xu, Shumin Deng, and Huajun Chen. Mllm can see? dynamic correction decoding for hallucination mitigation. In *ICLR*, 2025. 2, 3, 7

[72] Fei Wang, Xingchen Wan, Ruoxi Sun, Jiefeng Chen, and Sercan O Arik. Astute rag: Overcoming imperfect retrieval augmentation and knowledge conflicts for large language models. In *ACL*, 2025. 2, 3

[73] Jiachen Tianhao Wang, Tong Wu, Dawn Song, Prateek Mittal, and Ruoxi Jia. Greats: Online selection of high-quality data for llm training in every iteration. *NeurIPS*, 2024. 6, 1

[74] Xiuying Wei, Skander Moalla, Razvan Pascanu, and Caglar Gulcehre. Building on efficient foundations: Effective training of llms with structured feedforward layers. *NeurIPS*, 37, 2024. 1

[75] Sangmin Woo, Donguk Kim, Jaehyuk Jang, Yubin Choi, and Changick Kim. Don't miss the forest for the trees: Attentional vision calibration for large vision language models. In *ACL Findings*, 2025. 2

[76] Guangxuan Xiao, Yuandong Tian, Beidi Chen, Song Han, and Mike Lewis. Efficient streaming language models with attention sinks. *arXiv:2309.17453*, 2023. 4

[77] Chunzhao Xie, Tongxuan Liu, Lei Jiang, Yuting Zeng, Yunheng Shen, Weizhe Huang, Jing Li, Xiaohua Xu, et al. Tarac: Mitigating hallucination in lvlms via temporal attention real-time accumulative connection. *arXiv:2504.04099*, 2025. 3

[78] Chenghao Xu, Lyu Guangtao, Yan Jiexi, Yang Muli, and Cheng Deng. Llm knows body language, too: Translating speech voices into human gestures. In *ACL*, 2024. 2

[79] An Yang, Anfeng Li, Baosong Yang, Beichen Zhang, Binyuan Hui, Bo Zheng, Bowen Yu, Chang Gao, Chenguang Huang, Chenxu Lv, et al. Qwen3 technical report. *arXiv:2505.09388*, 2025. 2

[80] Yunzhi Yao, Ningyu Zhang, Zekun Xi, Mengru Wang, Ziwen Xu, Shumin Deng, and Huajun Chen. Knowledge circuits in pretrained transformers. *NeurIPS*, 2024. 2

[81] Qinghao Ye, Haiyang Xu, Jiabo Ye, Ming Yan, Anwen Hu, Haowei Liu, Qi Qian, Ji Zhang, and Fei Huang. mplug-owl2: Revolutionizing multi-modal large language model with modality collaboration. In *CVPR*, 2024. 2, 1

[82] Shukang Yin, Chaoyou Fu, Sirui Zhao, Tong Xu, Hao Wang, Dianbo Sui, Yunhang Shen, Ke Li, Xing Sun, and Enhong Chen. Woodpecker: Hallucination correction for multimodal large language models. *arXiv:2310.16045*, 2023. 1

[83] Zeping Yu and Sophia Ananiadou. Neuron-level knowledge attribution in large language models. In *EMNLP*, 2024. 1

[84] Zihao Yue, Liang Zhang, and Qin Jin. Less is more: Mitigating multimodal hallucination from an eos decision perspective. In *ACL*, 2024. 1, 2

[85] Xiaofeng Zhang, Yihao Quan, Chaochen Gu, Chen Shen, Xiaosong Yuan, Shaotian Yan, Hao Cheng, Kaijie Wu, and Jieping Ye. Seeing clearly by layer two: Enhancing attention heads to alleviate hallucination in lvlms. *arXiv:2411.09968*, 2024. 1

[86] Xiaofeng Zhang, Yihao Quan, Chen Shen, Xiaosong Yuan, Shaotian Yan, Liang Xie, Wenxiao Wang, Chaochen Gu, Hao Tang, and Jieping Ye. From redundancy to relevance: Information flow in lvlms across reasoning tasks. In *ACL*, 2025. 3

[87] Hanzhang Zhou, Zijian Feng, Zixiao Zhu, Junlang Qian, and Kezhi Mao. Unibias: Unveiling and mitigating llm bias through internal attention and ffn manipulation. *NeurIPS*, 37, 2024. 1

[88] Yiyang Zhou, Chenhang Cui, Jaehong Yoon, Linjun Zhang, Zhun Deng, Chelsea Finn, Mohit Bansal, and Huaxiu Yao. Analyzing and mitigating object hallucination in large vision-language models. In *ICLR*, 2024. 1

[89] Deyao Zhu, Jun Chen, Xiaoqian Shen, Xiang Li, and Mohamed Elhoseiny. Minigpt-4: Enhancing vision-language understanding with advanced large language models. *arXiv:2304.10592*, 2023. 2, 1

[90] Xin Zou, Yizhou Wang, Yibo Yan, Sirui Huang, Kening Zheng, Junkai Chen, Chang Tang, and Xuming Hu. Look twice before you answer: Memory-space visual retracing for hallucination mitigation in multimodal large language models. In *ICML*, 2025. 2, 3

# Revealing Perception and Generation Dynamics in LVLMs: Mitigating Hallucinations via Validated Dominance Correction

## Supplementary Material

### A. More Examples

We show multiple examples of both correct and hallucination predictions in Figs. 13, 14, 15, 16, 17, 18, 19, and 20.

From the perception perspective, the model consistently follows the **GATE** pattern: it first attends to the overall scene (Global), then gradually approaches the target region (Approach), focuses tightly on the relevant area (Tighten), and finally explores nearby regions (Explore).

From the token generation perspective, sudden shifts in the final one or two layers frequently occur. In hallucinated examples, the final output tokens often never appear as dominant (rank-1) tokens in either the attention or FFN streams. Instead, they repeatedly appear among subdominant tokens (ranks 2–5) and, through accumulation across layers, eventually become dominant. This observation further supports the **SAD** pattern, where subdominant, partially incorrect tokens gradually overtake previously correct dominant predictions.

Leveraging these insights, we propose **VDC** to detect and mitigate hallucinations. VDC identifies tokens that fail to receive validation from either visual perception (attention) or internal knowledge (FFN) and replaces them with previously validated dominant tokens, thereby reducing hallucination outputs and improving model reliability.

### B. Evaluation on More Methods and Models

To further verify the generality and robustness of VDC, we extend our evaluation to a broader set of **hallucination mitigation methods**, including DoLA [14], OPERA [28], VCD [42], Woodpecker [82], LURE [88], HALC [12], CODE [38], EAH [85], and VHR [24], as well as diverse **LVLM architectures**, including **MiniGPT-4** [89], **mPLUG-Owl2** [81], and the more recent and stronger **LLaVA-NeXT** [49]. As shown in Tab 8 and 7, VDC consistently achieves the lowest CHAIRs and CHAIRi scores, demonstrating its effectiveness across model architectures.

### C. Additional Observations

**Token Dynamics and Sample Difficulty.** Beyond the GATE (perception) and SAD (generation) phenomena, we observe clear layer-wise dynamics in dominant token evolution (Figs. 13–20, panel e). Early layers show frequent token fluctuations, whereas later layers reveal a natural separation between easy and difficult tokens. Simple or common tokens stabilize quickly, reflecting straightforward predictions, while complex or semantically rich tokens continue

Table 7. Results of MiniGPT-4 and mPLUG-Owl2 on CHAIR with a maximum token length of 64, following the HALC setting.

Method	MiniGPT-4		mPLUG-Owl2	
	CHAIRs ↓	CHAIRi ↓	CHAIRs ↓	CHAIRi ↓
DoLA	30.87 ± 5.52	11.70 ± 0.13	24.60 ± 0.24	8.73 ± 0.30
OPERA	30.00 ± 4.43	11.67 ± 0.22	22.13 ± 0.86	7.57 ± 1.22
VCD	30.27 ± 0.44	12.60 ± 0.45	27.27 ± 7.32	9.73 ± 1.22
Woodpecker	28.87 ± 2.20	10.20 ± 0.85	26.33 ± 1.98	8.43 ± 0.80
LURE	27.88 ± 2.25	10.20 ± 0.85	21.27 ± 0.06	7.67 ± 0.11
HALC	17.80 ± 0.03	8.10 ± 0.14	17.33 ± 4.30	7.43 ± 0.11
<b>VDC (ours)</b>	<b>14.68 ± 0.04</b>	<b>7.42 ± 0.12</b>	<b>15.58 ± 4.52</b>	<b>6.84 ± 0.12</b>

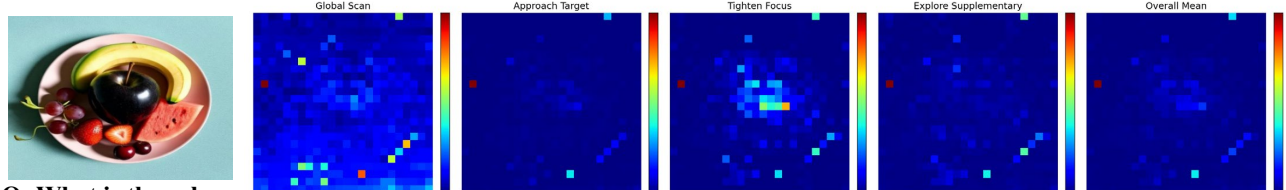
Table 8. Results of the newer and stronger LLaVA-NeXT with a maximum token length of 128, following the VHR setting.

Method	CHAIRs ↓	CHAIRi ↓
DoLa	28.76±2.58	8.12±0.78
VCD	30.80±2.48	8.72±0.94
CODE	27.84±2.73	7.98±0.92
EAH	28.13±1.13	6.62±0.49
VHR	24.96±2.09	6.80±0.59
<b>VDC (ours)</b>	<b>20.84±1.62</b>	<b>6.28±0.54</b>

to fluctuate, indicating higher uncertainty and stronger reasoning requirements. This stabilization pattern provides actionable signals for both efficiency and sample difficulty estimation. Tokens that stabilize early can be safely skipped in later computation, enabling potential acceleration via adaptive early-exit or selective inference [18, 37, 61]. Persistently fluctuating tokens highlight harder instances, which can guide dataset curation, focused training, or targeted evaluation [7, 9, 73]. Beyond hallucination analysis, these insights may also benefit other multimodal tasks involving token-level uncertainty, such as curriculum learning, active learning, or adaptive inference strategies.

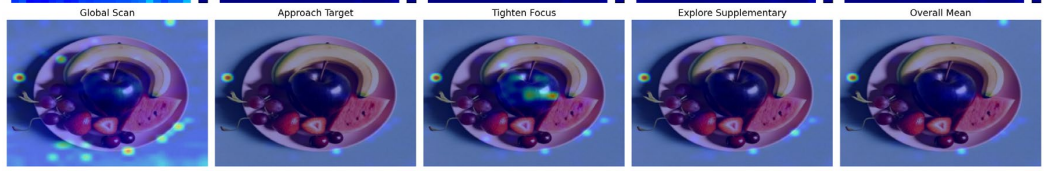
**Submodule Functional Roles.** Analysis of attention (panel g) and FFN outputs (panel h) further suggests distinct functional roles [8, 39, 40, 74, 83, 87]. FFN outputs often contain incomplete or auxiliary tokens, such as grammatical connectors or contextual fillers, whereas attention outputs produce semantically grounded and visually aligned tokens, including nouns, verbs, and adjectives. This pattern indicates that attention primarily supports content grounding, while FFN contributes to linguistic refinement and contextual coherence, potentially reflecting a complementary division of labor in LVLM decoding. Further research is needed to validate and generalize this observation.

Overall, our unified perception–generation analysis reveals internal dynamic processes that static attention or attribution metrics fail to capture, offering deeper mechanistic understanding and practical guidance for building more interpretable and reliable LVLMs.



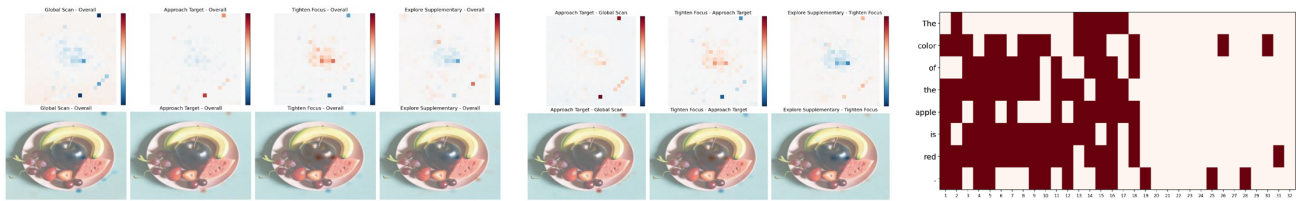
Q: What is the color of the apple?

A: The color of the apple is red.

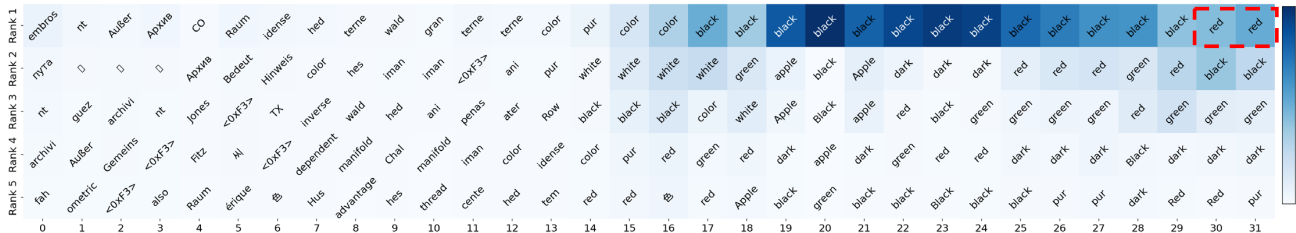


(a) Example

(b) Heatmaps of visual attention across different stages



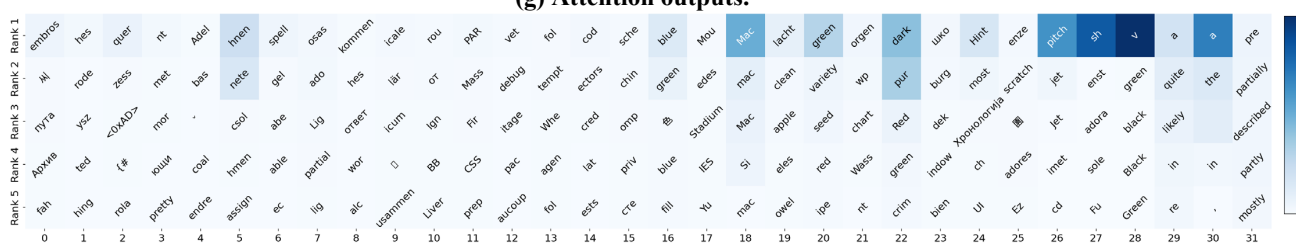
(c) Stage-to-global attention difference maps. (d) Inter-stage attention difference maps. (e) Dominant token changes.



(d) Inter-stage attention difference maps.



(e) Dominant token changes.



(f) Layer outputs.

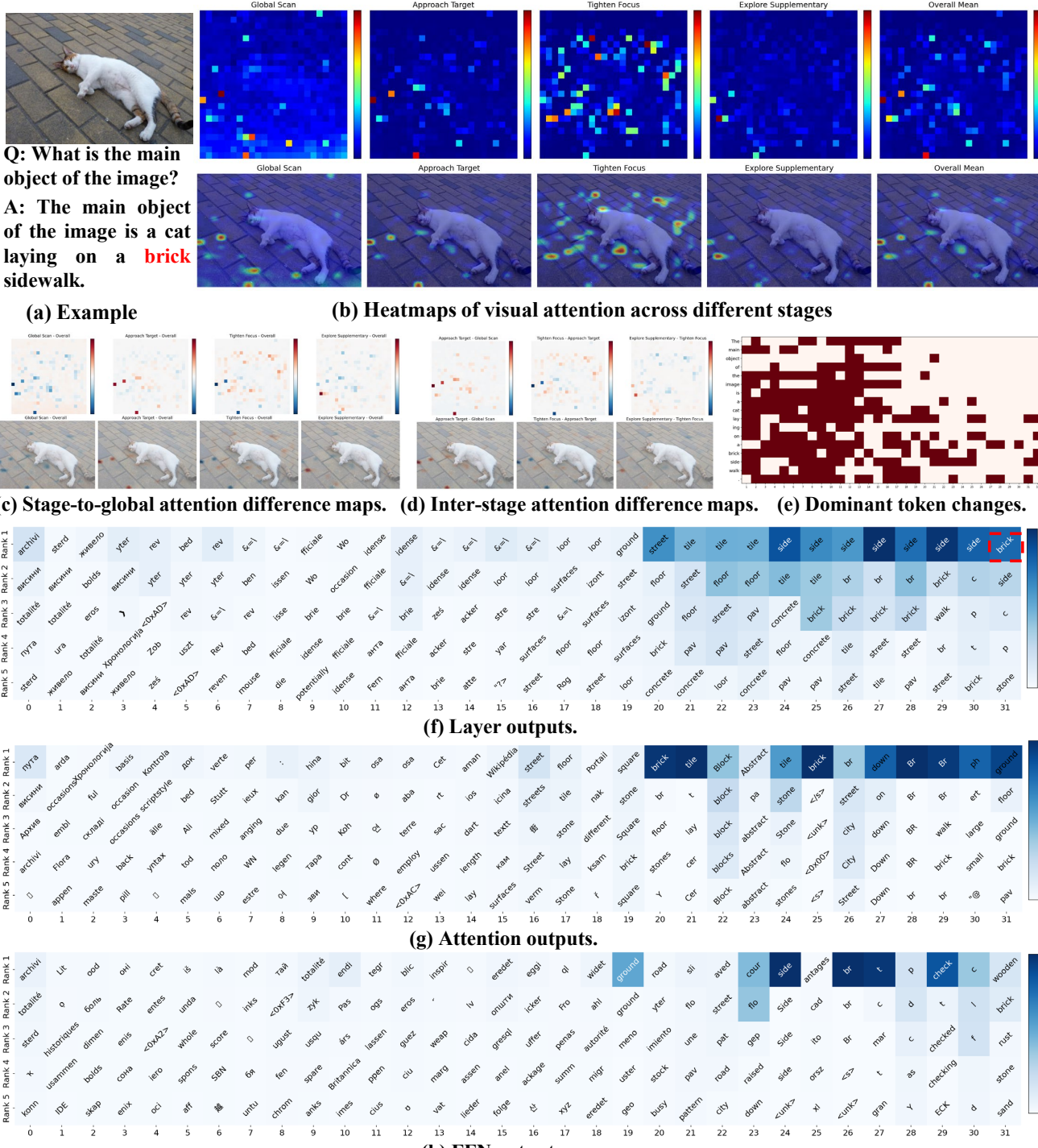


(g) Attention outputs.

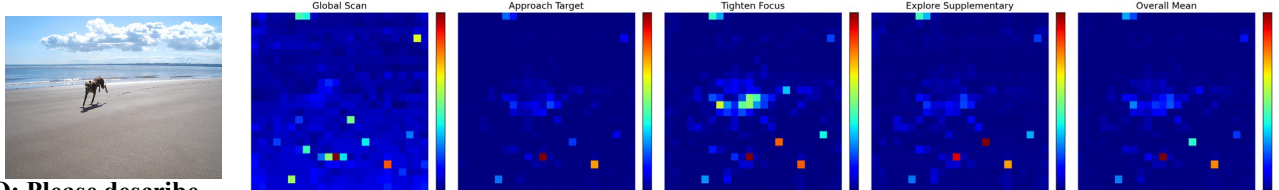


(h) FFN outputs.

Figure 13. An example of a sudden shift occurring in the last two layers. From the perception perspective, during the Tighten phase, the model correctly attends to the target region. From the token generation perspective, the model produces the correct token “black” in intermediate layers but shifts to the incorrect token “red” in the final two layers. As shown in panels (f) (g) and (h), the token “red” never appears as the dominant (rank-1) token in either the attention or FFN streams, but frequently appears among subdominant tokens (ranks 2–5). Through repeated accumulation, these subdominant signals gradually dominate, resulting in the incorrect output and illustrating the SAD pattern.



**(h) FFN outputs.**  
 Figure 14. A right example of a sudden shift in the final layer. During token generation, the model outputs the token “brick” at the last layer, which has already appeared as a dominant token in the attention stream, thus requiring no correction. Other tokens such as “side” and “tile” are also correct, but “brick” is more challenging and demonstrates higher precision. This indicates that not all late-layer sudden shifts are erroneous, highlighting the necessity of the last several layers. Therefore, we term the last stage *Explore Supplementary*. From the perception perspective, the model first attends to the overall scene (Global), then gradually approaches the brick regions near the cat (Approach), focuses tightly on the surrounding bricks (Tighten), and finally explores nearby areas (Explore). (e) further illustrates that the dynamics of sudden shifts vary with token difficulty: simple tokens such as “the,” “main,” and “object” stabilize quickly, whereas more complex tokens like “laying,” “brick,” and “side” continue to fluctuate across layers.



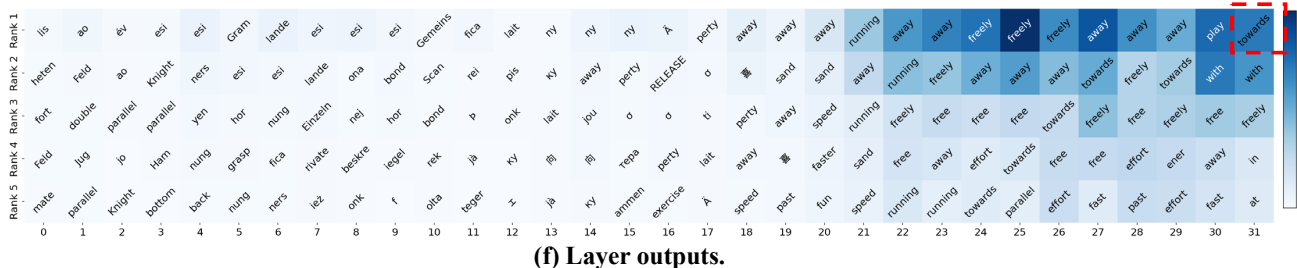
**Q:** Please describe this image in detail.  
**A:** ...The dog appears to be running **towards** the water, possibly to cool off.

### (a) Example

### (b) Heatmaps of visual attention across different stages



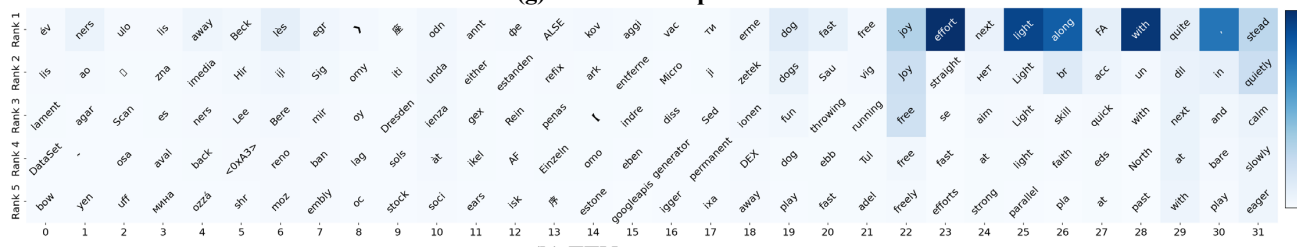
**(c) Stage-to-global attention difference maps. (d) Inter-stage attention difference maps. (e) Dominant token changes.**



### (f) Layer outputs.

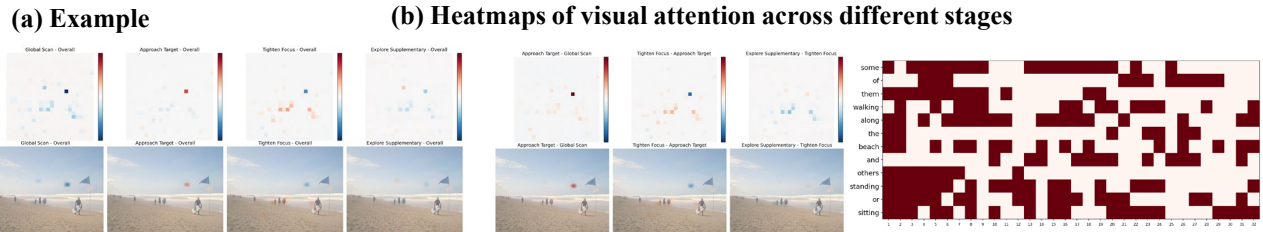
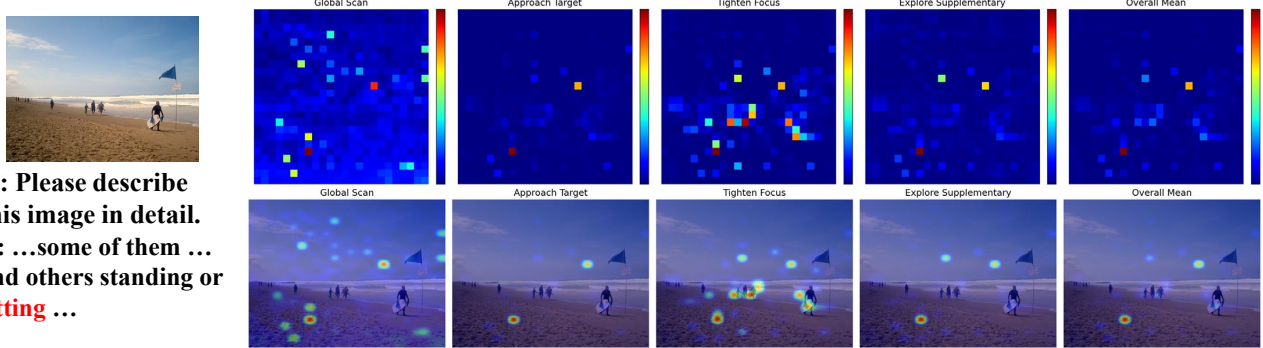


### (g) Attention outputs



(h) FFN outputs.

Figure 15. A hallucination example of a sudden shift in the final layer. From the perception perspective, during the Tighten phase, the model correctly attends to the target region. From the token generation perspective, the model produces the correct token “away” in intermediate layers but shifts to the incorrect token “towards” in the final layer. As shown in panels (f) (g) and (h), the token “towards” never appears as the dominant (rank-1) token in either the attention or FFN streams, but frequently appears among subdominant tokens (ranks 2–5). Through repeated accumulation, these subdominant signals gradually dominate, resulting in the incorrect output and illustrating the **SAD** pattern.



**(c) Stage-to-global attention difference maps. (d) Inter-stage attention difference maps. (e) Dominant token changes.**

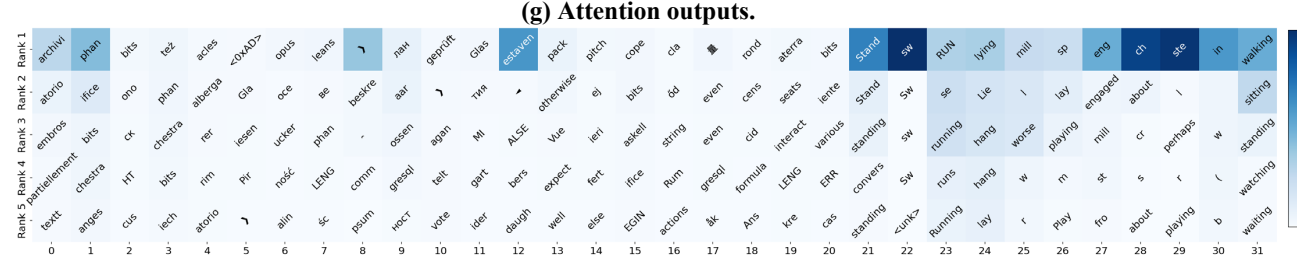
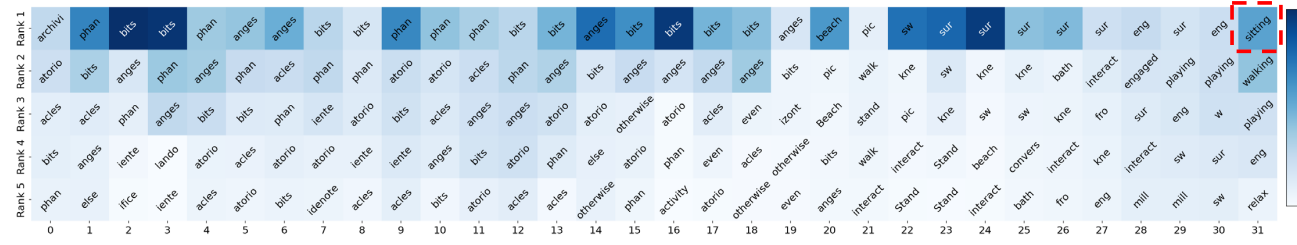


Figure 16. A hallucination example of a sudden shift in the final layer. From the perception perspective, during the Tighten phase, the model correctly attends to the target region. From the token generation perspective, the model produces the correct token “sur” in intermediate layers but shifts to the incorrect token “sitting” in the final layer. As shown in panels (f) (g) and (h), the token “sitting” never appears as the dominant (rank-1) token in either the attention or FFN streams, but frequently appears among subdominant tokens (ranks 2–5). Through repeated accumulation, these subdominant signals gradually dominate, resulting in the incorrect output and illustrating the **SAD** pattern.

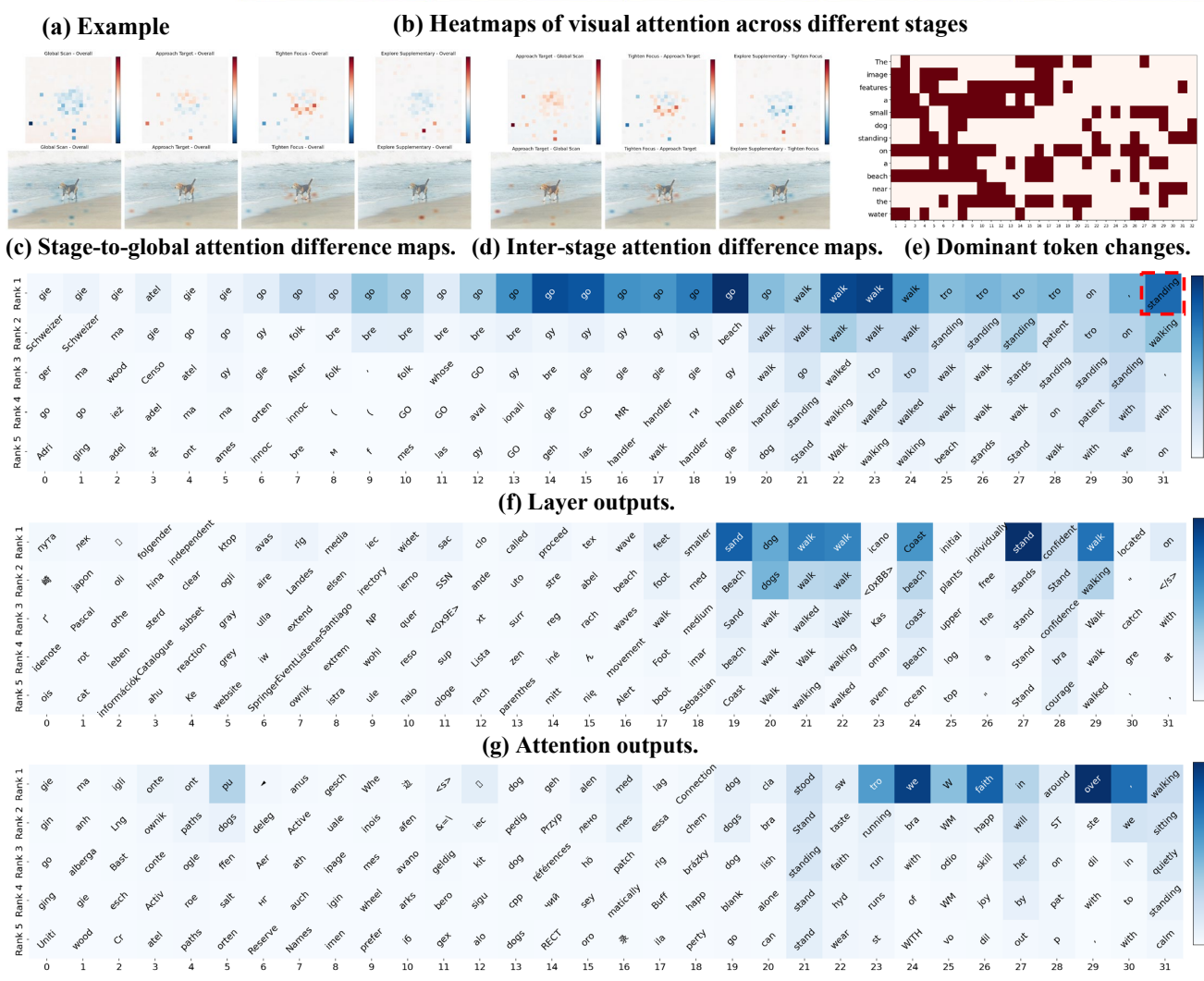
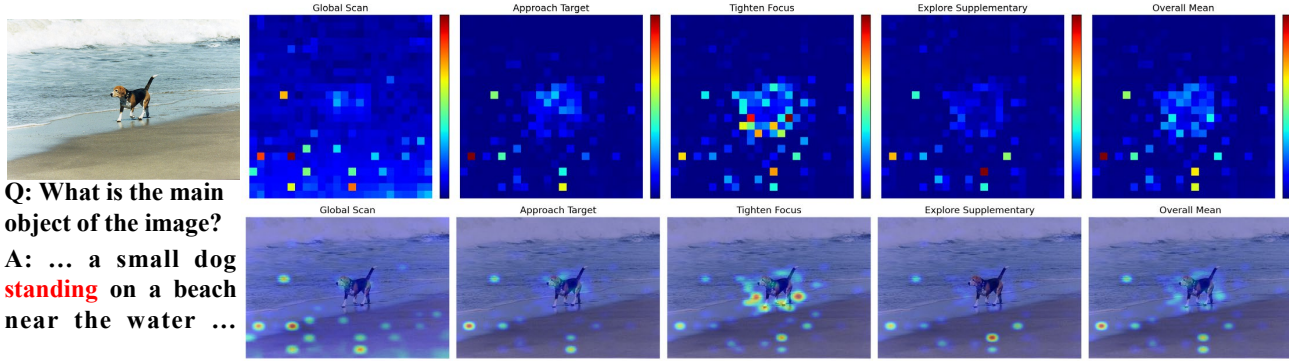
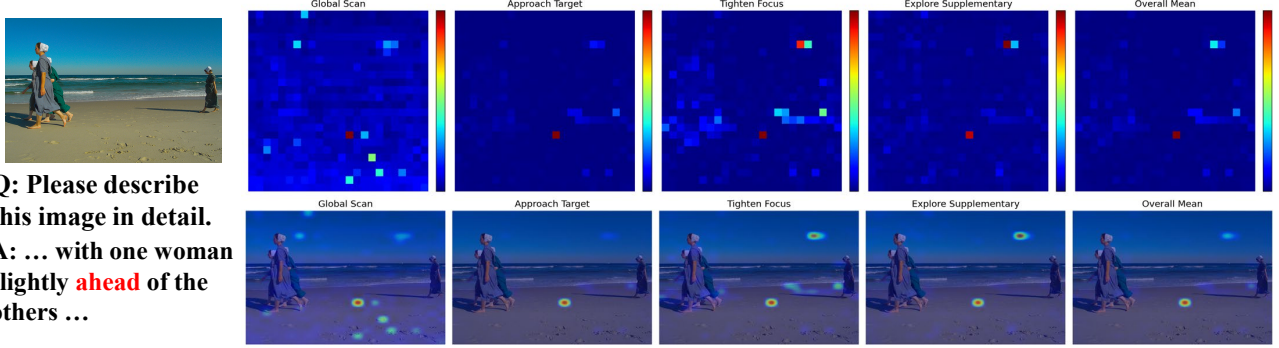
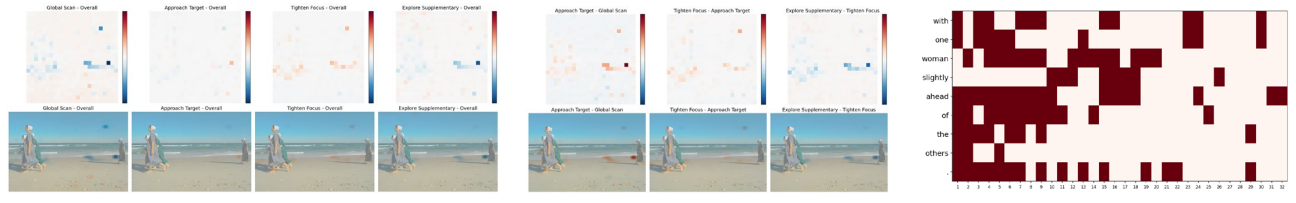


Figure 17. An hallucination example of a sudden shift in the final layer. From the perception perspective, during the Tighten phase, the model correctly attends to the target region. From the token generation perspective, the model produces the correct tokens (“go”, “walk”, “tro”) in intermediate layers but shifts to the incorrect token “standing” in the final layer. As shown in panels (f) (g) and (h), the token “standing” never appears as the dominant (rank-1) token in either the attention or FFN streams, but frequently appears among subdominant tokens (ranks 2–5). Through repeated accumulation, these subdominant signals gradually dominate, resulting in the incorrect output and illustrating the **SAD** pattern.

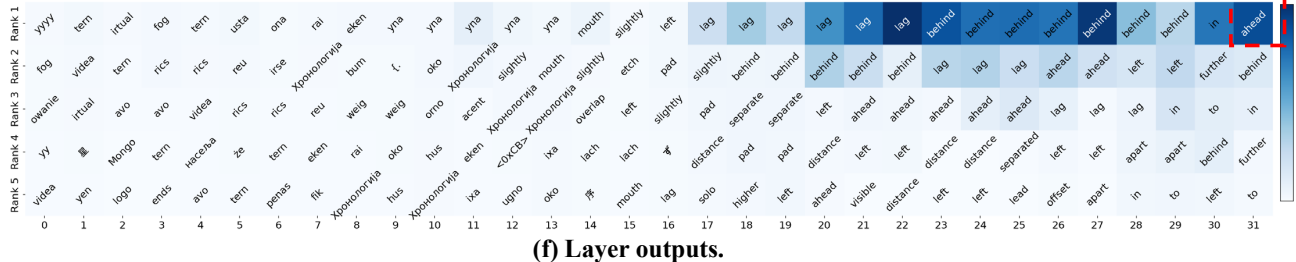


**(a) Example**

**(b) Heatmaps of visual attention across different stages**



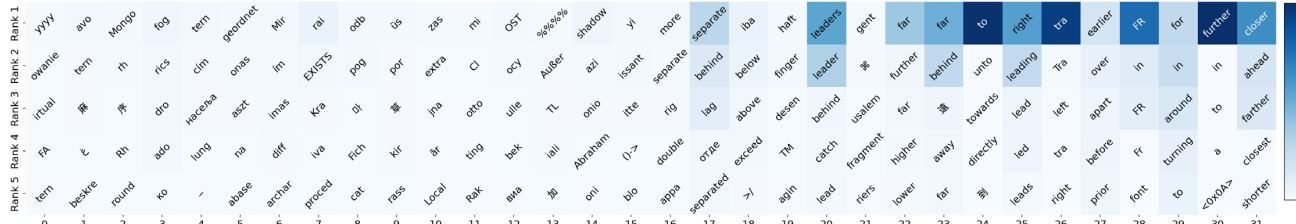
**(c) Stage-to-global attention difference maps. (d) Inter-stage attention difference maps. (e) Dominant token changes.**



**(f) Layer outputs.**

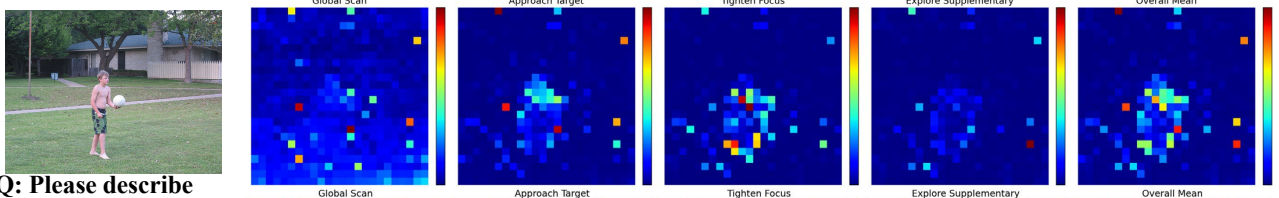


**(g) Attention outputs.**



**(h) FFN outputs.**

Figure 18. A hallucination example of a sudden shift in the final layer. From the perception perspective, during the Tighten phase, the model correctly attends to the target region. From the token generation perspective, the model produces the correct token “behind” in intermediate layers but shifts to the incorrect token “ahead” in the final layer. As shown in panels (f) (g) and (h), the token “ahead” never appears as the dominant (rank-1) token in either the attention or FFN streams, but frequently appears among subdominant tokens (ranks 2–5). Through repeated accumulation, these subdominant signals gradually dominate, resulting in the incorrect output and illustrating the SAD pattern.



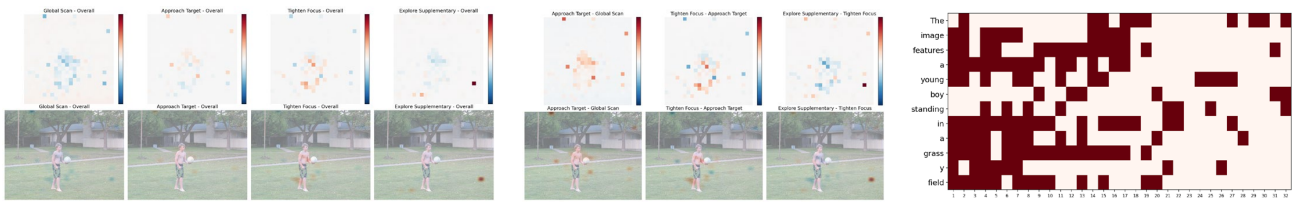
**Q: Please describe this image in detail.**

**A: ... a young boy **standing** in a grassy field ...**

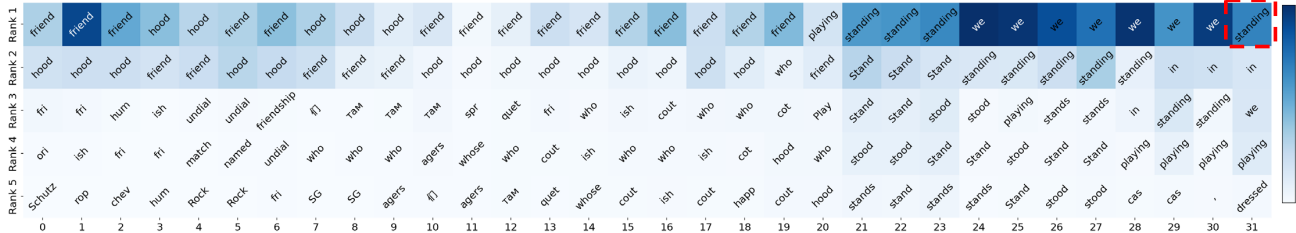


**(a) Example**

**(b) Heatmaps of visual attention across different stages**



**(c) Stage-to-global attention difference maps. (d) Inter-stage attention difference maps. (e) Dominant token changes.**



**(f) Layer outputs.**

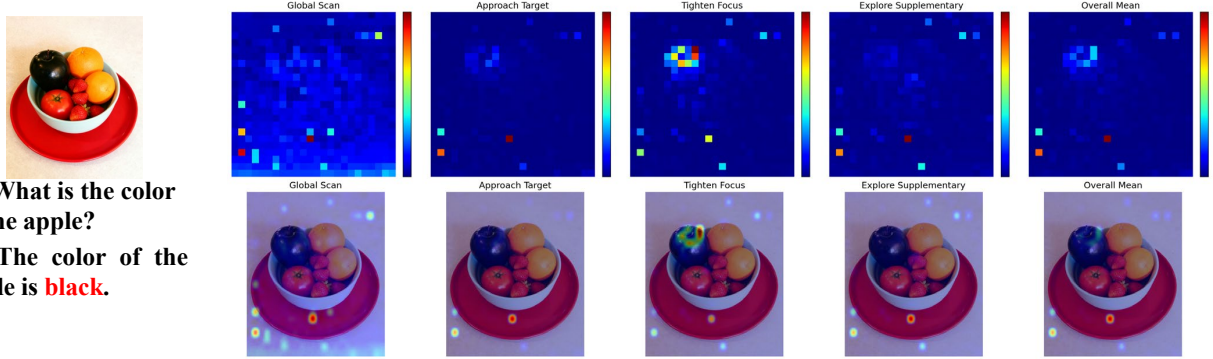


**(g) Attention outputs.**



**(h) FFN outputs.**

Figure 19. A right example illustrating the role of the FFN in token generation. The model outputs the token “standing” at the final layer. While the attention stream primarily predicts “stand,” the FFN stream captures the correct grammatical form “standing,” reflecting its role in enhancing syntax-related information. The overall visual attention still follows the GATE pattern.

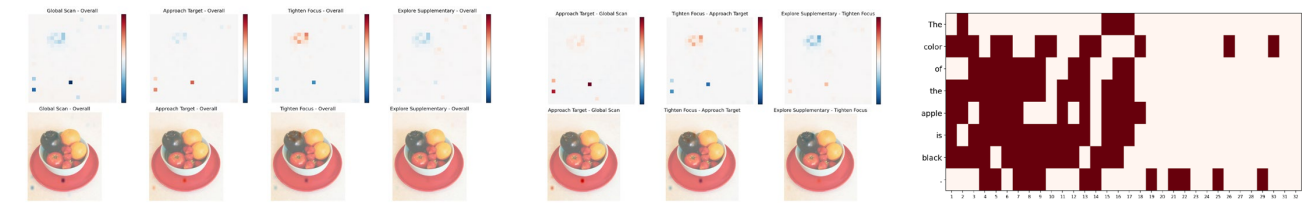


**Q: What is the color of the apple?**

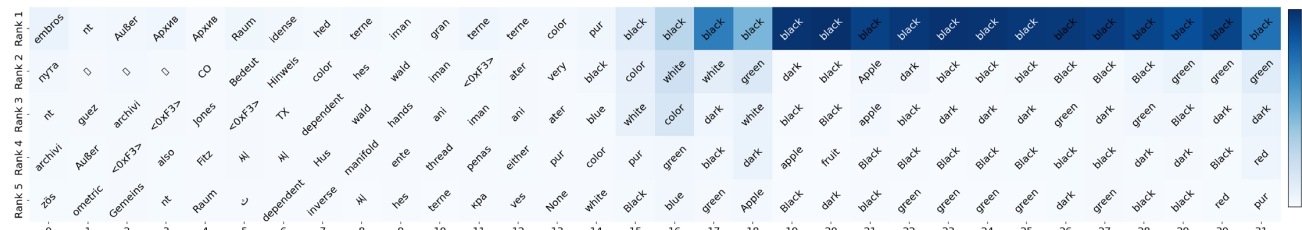
**A: The color of the apple is black.**

**(a) Example**

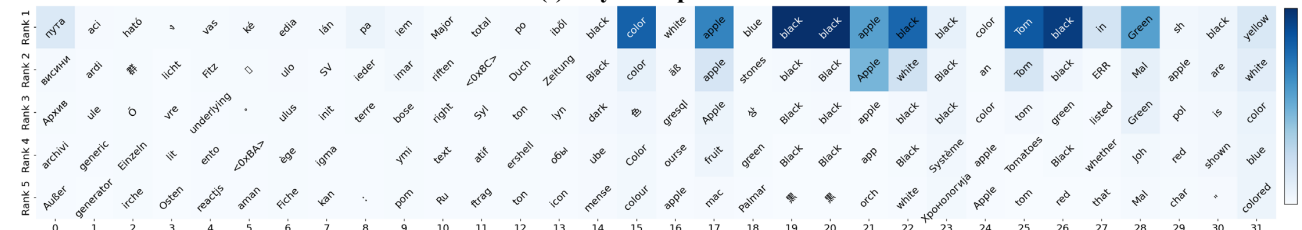
**(b) Heatmaps of visual attention across different stages**



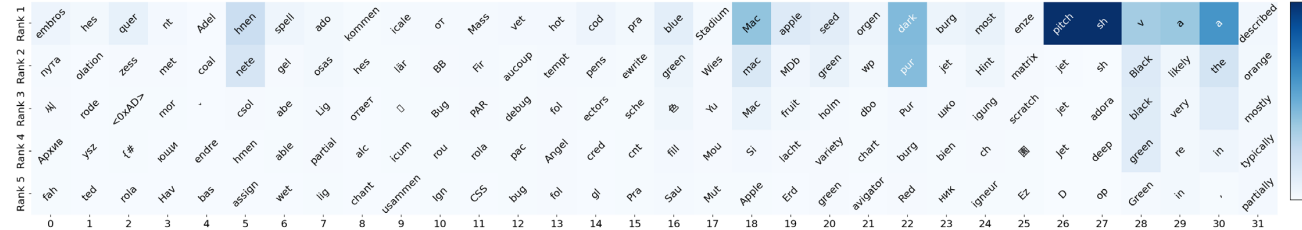
**(c) Stage-to-global attention difference maps. (d) Inter-stage attention difference maps. (e) Dominant token changes.**



**(f) Layer outputs.**



**(g) Attention outputs.**



**(h) FFN outputs.**

Figure 20. An example where the model correctly predicts the color of the apple as “black,” despite strong surrounding distractions. This demonstrates that the failure in Figure 13 is not due to the model’s inability to learn the “black apple” association, but rather a result of internal mechanism issues. The visual attention follows the GATE pattern: the model first attends to the overall scene (Global), then gradually approaches the apple region (Approach), tightly focuses on the apple itself (Tighten), and finally explores nearby areas (Explore). During generation, the token “black” remains consistently predicted across layers and appears as a dominant token in the attention stream. According to VDC, this indicates that “black” has been validated and requires no correction.